JOURNAL OF GEOPHYSICAL RESEARCH, VOL. 117, D23301, doi:10.1029/2011JD016911, 2012

Southern Hemisphere Additional Ozonesondes (SHADOZ) ozone climatology (2005–2009): Tropospheric and tropical tropopause layer (TTL) profiles with comparisons to OMI-based ozone products

Anne M. Thompson,[1] Sonya K. Miller,[1] Simone Tilmes,[2] Debra W. Kollonige,[1] Jacquelyn C. Witte,[3,4] Samuel J. Oltmans,[5,6] Bryan J. Johnson,[5] Masatomo Fujiwara,[7] F. J. Schmidlin,[8] G. J. R. Coetzee,[9] Ninong Komala,[10] Matakite Maata,[11] Maznorizan bt Mohamad,[12] J. Nguyo,[13] C. Mutai,[13] S-Y. Ogino,[14,15] F. Raimundo Da Silva,[16] N. M. Paes Leme,[16] Francoise Posny,[17] Rinus Scheele,[18] Henry B. Selkirk,[19] Masato Shiotani,[20] René Stübi,[21] Gilbert Levrat,[21] Bertrand Calpini,[21] Valérie Thouret,[22] Haruo Tsuruta,[23] Jessica Valverde Canossa,[24] Holger Vömel,[25] S. Yonemura,[26] Jorge Andrés Diaz,[27] Nguyen T. Tan Thanh,[28] and Hoang T. Thuy Ha[28]

[1]   We present a regional and seasonal climatology of SHADOZ ozone profiles in the troposphere and tropical tropopause layer (TTL) based on measurements taken during the first five years of Aura, 2005–2009, when new stations joined the network at Hanoi, Vietnam; Hilo, Hawaii; Alajuela/Heredia, Costa Rica; Cotonou, Benin. In all, 15 stations operated during that period. A west-to-east progression of decreasing convective influence and increasing pollution leads to distinct tropospheric ozone profiles in three regions: (1) western Pacific/eastern Indian Ocean; (2) equatorial Americas (San Cristóbal, Alajuela, Paramaribo); (3) Atlantic and Africa. Comparisons in total ozone column from soundings, the Ozone Monitoring Instrument (OMI, on Aura, 2004-) satellite and ground-based instrumentation are presented. Most stations show better agreement with OMI than they did for EP/TOMS comparisons (1998–2004; Earth-Probe/Total Ozone Mapping Spectrometer), partly due to a revised above-burst ozone climatology. Possible station biases in the stratospheric segment of the ozone measurement noted in the first 7 years of SHADOZ ozone profiles are re-examined. High stratospheric bias observed during the

---

[1]Department of Meteorology, Pennsylvania State University, University Park, Pennsylvania, USA.
[2]Atmospheric Chemistry Division, NCAR, Boulder, Colorado, USA.
[3]SSAI, Lanham, Maryland, USA.
[4]Also at NASA Goddard Space Flight Center, Greenbelt, Maryland, USA.
[5]Global Monitoring Division, NOAA ESRL, Boulder, Colorado, USA.
[6]Also at CIRES, University of Colorado Boulder, Boulder, Colorado, USA.
[7]Faculty of Environmental Earth Science, Hokkaido University, Sapporo Japan.
[8]NASA Wallops Flight Facility, Wallops Island, Virginia, USA.
[9]South Africa Weather Service, Pretoria, South Africa.
[10]National Institute of Aeronautics and Space, Bandung, Indonesia.
[11]School of Biological and Chemical Sciences, Division of Chemistry, University of the South Pacific, Suva, Fiji.
[12]Malaysian Meteorological Department, Ministry of Science, Technology and Innovation, Petaling Jaya, Malaysia.
[13]Kenya Meteorological Department, Nairobi, Kenya.

Corresponding author: A. M. Thompson, Department of Meteorology, Pennsylvania State University, 503 Walker Bldg., University Park, PA 16802-5013, USA. (amt16@psu.edu)

[14]Monsoon Hydrological Cycle Research Team, Tropical Climate Variations Research Program, Research Institute for Global Change, Japan Agency for Marine-Earth Science and Technology, Yokosuka, Japan.
[15]Also at Graduate School of Science, Kobe University, Kobe, Japan.
[16]INPE, São José dos Campos, Brazil.
[17]Université de la Réunion, Saint Denis, France.
[18]Royal Netherlands Meteorological Institute, de Bilt, Netherlands.
[19]Universities Space Research Association, Columbia, Maryland, USA.
[20]Research Institute for Sustainable Humanosphere, Kyoto University, Kyoto, Japan.
[21]MeteoSwiss Aerological Station, Federal Office of Meteorology and Climatology, Payerne, Switzerland.
[22]Laboratoire d'Aérologie, Université de Toulouse, CNRS, Toulouse, France.
[23]Division of Climate System Research, Atmosphere and Ocean Research Institute, University of Tokyo, Kashiwa, Japan.
[24]Department of Environmental Sciences, Universidad Nacional, Heredia, Costa Rica.
[25]GRUAN Lead Centre, Deutscher Wetterdienst, Lindenberg, Germany.
[26]National Institute for Agro-Environmental Sciences, Tsukuba, Japan.
[27]Gas Sensing Laboratory, CICANUM, Physics School, Universidad de Costa Rica, San Jose, Costa Rica.
[28]Aero-Meteorological Observatory, National Hydro-Meteorological Services, Ministry of Natural Resources and Environment, Hanoi, Vietnam.

TOMS period appears to persist at one station. Comparisons of SHADOZ tropospheric ozone and the daily Trajectory-enhanced Tropospheric Ozone Residual (TTOR) product (based on OMI/MLS) show that the satellite-derived column amount averages 25% low. Correlations between TTOR and the SHADOZ sondes are quite good (typical r^2 = 0.5–0.8), however, which may account for why some published residual-based OMI products capture tropospheric interannual variability fairly realistically. On the other hand, no clear explanations emerge for why TTOR-sonde discrepancies vary over a wide range at most SHADOZ sites.

1. Introduction

1.1. SHADOZ Background and Scientific Overview

[2] The Southern Hemisphere Additional Ozonesonde Network (SHADOZ, http://croc.gsfc.nasa.gov/shadoz) was initiated in 1998 as an international partnership with both technological and scientific goals related to the collection of ozone profiles in the troposphere up to the mid-stratosphere [*Thompson et al.*, 2003a, 2011a, 2011b].

[3] The original spatial coverage of SHADOZ was determined by two factors: (1) a requirement that the network consist of existing stations; (2) full zonal coverage to resolve the equatorial "wave-one" feature observed in satellite total ozone [*Fishman and Larsen*, 1987; *Shiotani*, 1992; *Kim et al.*, 1996; *Thompson et al.*, 2003b]. In 1998 the nine known stations meeting these criteria were in the southern hemisphere, hence the SHADOZ name [*Thompson et al.*, 2003a]. The characterization of an "ozone paradox" [*Thompson et al.*, 2000; *Martin et al.*, 2002; *Sauvage et al.*, 2006], INDOEX (Indian Ocean Experiment, 1999) sampling [*Zachariasse et al.*, 2001], and a report from Kuala Lumpur [*Yonemura et al.*, 2002], led to the addition of sites north of the equator: Paramaribo (1999), Kuala Lumpur (joined 2002), Heredia, Costa Rica (2005), Cotonou (operated 2004–2007). Data from Hilo, Hawaii, and Hanoi, Vietnam, were added to the SHADOZ archive in 2009 and 2010, respectively. Stations operating in the past 8 years appear in Figure 1. More than 5000 sets of ozone and pressure-temperature-humidity (PTU) profiles are available at the SHADOZ website: http://croc.gsfc.nasa.gov/shadoz. The expectation that leveraging resources at operational stations would sustain SHADOZ [*Thompson et al.*, 2003a] has been realized; there are 13 sites active in the network although equipment shortages have caused interruptions at several stations since 2007.

[4] The initial motivation for SHADOZ was to ensure sufficient ozone profiles in the tropics and subtropics for validation of satellite instruments being launched around the turn of the century. These included Odin and Atmospheric Chemistry Experiment (Canadian, 2003-); Fourier Transform Spectrometer (ACE-FTS) (Figure 2), Scanning Imaging Absorption SpectroMeter for Atmospheric ChartographY (SCIAMACHY, 2002–2012) and Global Ozone Monitoring by Occultation of Stars (GOMOS) on ENVISAT [*Burrows et al.*, 2011] (Figure 2), four ozone sensors on Aura [*Jiang*, 2007; *Schoeberl et al.*, 2007; *Nardi et al.*, 2008;

Nassar et al., 2008; *Osterman et al.*, 2008] and GOME-2 (Global Ozone Monitoring Experiment GOME II, 2003- and 2012-) launched on METOP (2006 and 2012 in Figure 2). Continuous validation was enabled for the SBUV series on National Oceanic and Atmospheric Administration (NOAA) operational polar orbiters [*Bhartia et al.*, 2012] and the successor Ozone Mapping and Profiling Suite (OMPS) on the Suomi National Polar-Orbiting Partnership (NPP) satellite. Other instruments that have used SHADOZ for validation also appear in Figure 2. In addition to standard satellite products, sondes are used for evaluating profiles from specialized satellite retrievals [*Liu et al.*, 2010] and data assimilation [*Stajner et al.*, 2008].

[5] Chemical-transport models also rely on SHADOZ sondes for validation [*Martin et al.*, 2002; *Stevenson et al.*, 2006; *Kaminski et al.*, 2008] with the profiles particularly useful for evaluating ozone simulations near the tropopause [*Considine et al.*, 2008]. Climatologies that incorporate ozone data from SHADOZ have become the norm for validating the coupled chemistry-climate models [*Eyring et al.*, 2005] used in intercomparison exercises that support UNEP/WMO Ozone [*World Meteorological Organization (WMO)*, 2003, 2007, 2011] and *Intergovernmental Panel on Climate Change* [2007] Assessments.

[6] The geographical, vertical and temporal resolution of SHADOZ profiles have provided insights into tropical chemistry and dynamics not previously possible. For example, in the past 5–7 years, SHADOZ data have helped define the Tropical Tropopause Layer (TTL, also referred to as the Tropopause Transition Layer) [*Sherwood and Dessler*, 2003; *Folkins et al.*, 2002; *Fu et al.*, 2007; *Gettelman and Forster*, 2002; *Fueglistaler et al.*, 2009]. In *Randel et al.* [2007], SHADOZ data were used to show that maximum and minimum O_3 in the TTL differ by a factor of two, with annual variability related to the Brewer-Dobson cycle. *Konopka et al.* [2009] used SHADOZ data to argue that vertical transport is responsible for only part of the annual cycle, i.e. during boreal summer about 40% of lower stratospheric (LS) ozone variability is due to mixing -in from the extra-tropics.

[7] Investigations with SHADOZ ozone and temperature profiles show finer structure in the TTL due to the Quasi-biennial Oscillation (QBO) than can be observed with satellites [*Logan et al.*, 2003; cf. *Witte et al.*, 2008, Figure 1]. Indeed, *Lee et al.* [2010] used data from four equatorial SHADOZ stations to show that propagation of temperature and ozone anomalies from lower stratosphere (LS) to the

SHADOZ Sites
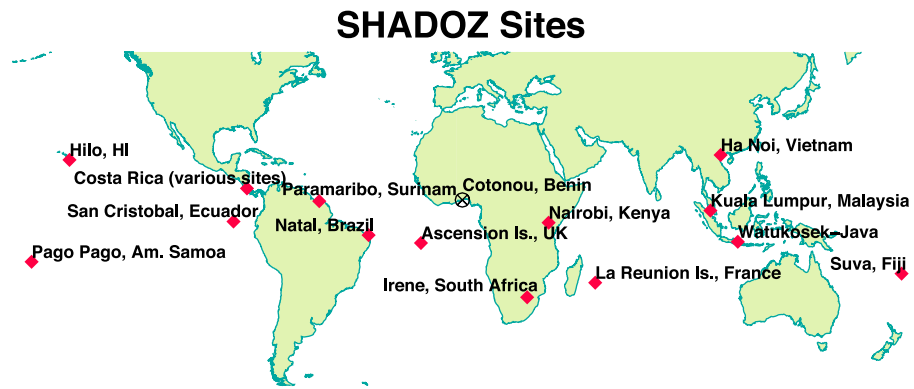
Figure 1. Map of SHADOZ stations that operated during the early Aura era, July 2004–2010. Malindi (ceased in 2006) is not included here. See operating period and technical summary for individual stations in Table 1. Technical details of SHADOZ sondes used at each site during 1998–2004, within the Earth-Probe/TOMS period, are given in *Thompson et al.* [2003a, 2007]. Tahiti operated in 1998–1999.

upper troposphere (UT) in response to QBO and El Niño–Southern Oscillation (ENSO) differ in both sign and timing from region to region. Similar ENSO anomalies for eight SHADOZ stations appear in *Randel and Thompson* [2011].

[8] Near daily ozonesonde launches over Panamá (Las Tablas, 7.8N, 80W) and the Alajuela (Costa Rica, 10°N, 84°W) SHADOZ site during a July-August 2007 field intensive, Tropical Composition, Clouds and Climate Coupling (TC4), linked active convection to wave initiation [*Thompson et al.*, 2010]. Four-times-daily radiosondes at Alajuela indicated convectively generated mixed Rossby-gravity waves above 14 km [*Selkirk et al.*, 2010]. Other studies of convective transport using SHADOZ data were made by *Folkins et al.* [2000, 2002] and *Mitovski et al*

[2012], who infer vertical mixing times from an S-shape in tropospheric ozone over Pacific SHADOZ stations and link them to annual cycles in temperature and tracers in the TTL [*Folkins et al.*, 2006]. *Fujiwara et al.* [1998, 2001] observed irreversible ozone transport from the tropical LS to UT due to breaking Kelvin waves generated by organized convection. Convection and related annual cycles in TTL and LS ozone for SHADOZ sites were also analyzed by *Takashima and Shiotani* [2007]. A small number of episodes in which very-low O_3 layers (<10 ppbv) at 100–300 hPa are observed at most SHADOZ stations is taken as a sign of deep convection over unpolluted sites or regions with halogen-depleted surface ozone [*Solomon et al.*, 2005; *Saiz-Lopez et al.*, 2011; cf. *Kley et al.*, 1996].
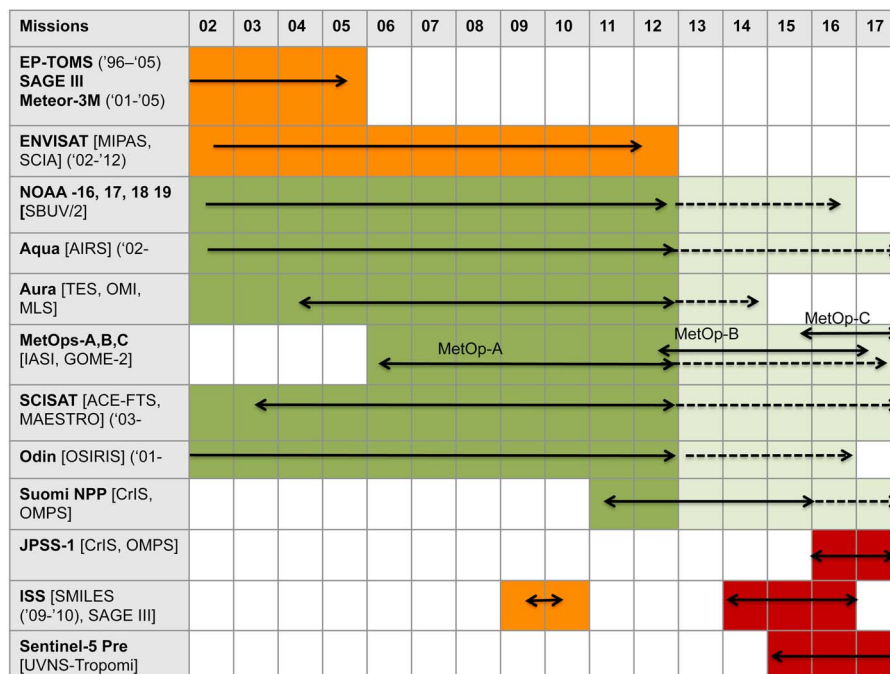
Figure 2. Timeline of satellite ozone instruments that have used SHADOZ for validation. Sensors of the past decade are indicated with expected lifetime of operational satellites (lighter shading) and several satellites planned for launch after 2015 by US, Canadian, European agencies and international partnerships.

Table 1. SHADOZ Station Locations Used in This Study, With Years of Record and Sample Number (SN) Analyzed for 2005–2009

Site	Latitude, Longitude	Years of SHADOZ Data	SN, 2005–2009
Cotonou[a]	7N, 15E	2005–2007	100
Irene[a]	25S, 28E	1999–2007	64
Nairobi	1S, 35E	1999–2010	189
La Réunion	21S, 55E	1998–2010	158
Hanoi	21N, 106E	2005–2009	106
Kuala Lumpur	2.7N, 102E	1998–2010	114
Watukosek	7.5S, 112.6E	1998–2010	65
Fiji[a]	18S, 178E	1998–2008	44
Hilo	19N, 157W	1998–2010	217
Am. Samoa	14S, 171W	1998–2010	157
Paramaribo	5N, 55W	1999–2009	140
Alajuela/Heredia	10N, 84W	2006–2010	192
San Cristóbal[a]	1S, 90W	1999–2008	103
Natal (Brazil)	6S, 35W	1998–2010	173
Ascension Is.	8S, 15W	1998–2010	207

[a]Gaps are significant at Fiji, Irene, San Cristóbal (launches interrupted in 2008, resumed in 2011). Cotonou operated from Dec. 2004 through Jan. 2007.

[9] Several recent papers have examined aspects of ozone variability in the free troposphere and TTL. Statistical clustering and trajectory analysis of profiles over two Atlantic SHADOZ stations [*Jensen et al.*, 2012] show strong correlation of vertical ozone structure with distinct meteorological conditions (cf. the Irene studies of *Diab et al.* [2004] and *Phahlane* [2007]). At Ascension, where convection is much less intense than over the Pacific stations, profiles with the lowest mean tropospheric ozone mixing ratio nonetheless display an S-shape during the most convectively period [*Jensen et al.*, 2012, Figure 3]. In *Thompson et al.* [2011a, 2011b] ozone and potential temperature laminae were used to identify gravity waves within the UT and TTL over 12 SHADOZ stations and to construct a gravity-wave index (GWI) that maximizes over the Pacific and eastern Indian Ocean and close to the Intertropical Convergence Zone (ITCZ), the inference being that convection initiates the waves.

[10] SHADOZ ozone and temperature data were used to compare three tropopause definitions among 9 SHADOZ stations for the purpose of determining the sensitivity of trends in tropopause height to the way the tropopause is defined [*Sivakumar et al.*, 2011]. In the latter study, the tropopause was used to separate the tropical region, defined as equatorward of 15°S, from the subtropics; no northern hemispheric SHADOZ stations were analyzed. A regionally classified ozone profile climatology based on sondes and aircraft profiles, prepared by *Tilmes et al.* [2012], features data from 1995 through 2009, including 9 SHADOZ stations. In addition to information on seasonal means, standard deviations, median and half-width, a diagnostic that describes similarly shaped probability distribution functions with reference to the profiles provides additional constraints for models and satellite retrievals.

1.2. Technological Overview of SHADOZ

[11] The technological objectives of SHADOZ are three-fold. First, SHADOZ set out to remedy a lack of consistent tropical ozone and PTU observations for validation of satellite ozone measurements in the tropics and sub-tropics. Consistency in this context refers to temporal

and geographical coverage. The temporal resolution is once per week at most sites (Figure 2; coordinates in Table 1). In addition to requirements for monitoring stratospheric ozone in the tropics, SHADOZ focused on measurements of tropospheric ozone by direct or indirect satellite observation. Residual-based and assimilation approaches to deriving tropospheric ozone from satellite observation have multiplied since the mid-1990s as data have become available from SCIAMACHY, GOME, ACE and on Aura.

[12] A second technological goal was the enhancement of speed and quantity in data distribution. All profiles collected at SHADOZ sites are distributed as soon as they are sent to the archive. Data dissemination is extended through sharing and/or web-links at the World Ozone and Ultraviolet Data Centre, Global Climate Observing System (GCOS), NDACC (Network for the Detection of Atmospheric Composition Change, http://www.ndacc.org) and the Aura Validation Data Center. SHADOZ stations participate in field campaigns with near-real-time data turn-around, e.g. the 2007 TC4 in Costa Rica [*Selkirk et al.*, 2010; *Thompson et al.*, 2010; *Toon et al.*, 2010].

[13] The beginning of SHADOZ coincided with a period of increasing attention to the ozonesonde technique as new laboratory studies were conducted [*Johnson et al.*, 2002; *Smit and Straeter*, 2004], instrument manufacturers updated instructions [*Komhyr*, 1986; *Komhyr et al.*, 1995] and the World Meteorological Organization (WMO) started developing procedures for new stations in the Global Atmospheric Watch (GAW) program. Thus, a third set of goals for SHADOZ emerged: raising standards of data quality through evaluation of the sonde instrument and operations; contributing to a consensus process for preferred technique; periodically evaluating potential instrumental effects as sonde climatologies are updated. For example, SHADOZ participants have helped raise accuracy and precision of the sonde measurement from ~15% to 5% from surface to mid-stratosphere [*WMO*, 2003, 2007, 2011]. However, comparisons of SHADOZ total ozone column amounts with co-located ground-based and satellite derived measurements [*Thompson et al.*, 2007, hereinafter T07] revealed station-to-station biases that appeared consistent with the variations in technique and instrument type employed in the network that were identified in the JOSIE (Jülich Ozonesonde Intercomparison Experiment; http://www.fz-juelich.de/icg/icg-2/josie) [*Smit et al.*, 2007] and Balloon Experiment on Standards for Ozone Sondes (BESOS) [*Deshler et al.*, 2008] intercomparison experiments.

1.3. Goals of This Paper

[14] Since the analysis in T07, four stations joined SHADOZ and Aura, with four ozone sensors onboard, was launched, providing OMI as a Back-scattered Ultraviolet (BUV)-based instrument suitable for comparing the more recent (September 2004 onward) sonde record to satellite overpasses. Two profile climatologies oriented toward BUV have been published since T07 [*McPeters et al.*, 2007; *McPeters and Labow*, 2012]. The latter study draws heavily on Microwave Limb Sounder (MLS; on UARS, 1991–2005; on Aura, 2004-) and profiles from all the SHADOZ stations. With more than 2000 profiles added to SHADOZ since 2006, tropospheric and TTL ozone profiles in the northern tropics, when zonally

averaged, increased up to 30% compared to *McPeters et al.* [2007] and earlier climatologies.

[15] The present study uses SHADOZ data from the OMI era. Section 3 presents an updated tropospheric and TTL climatology and addresses the following:

[16] 1. How do ozone distributions at two new subtropical stations, Hanoi and Hilo in the northern hemisphere, compare to those at the southern subtropical stations, Irene and La Réunion? How does ozone at the newer tropical stations, Cotonou and Alajuela/Heredia, compare to climatology at the longer-term stations in the Pacific, the Atlantic and Africa?

[17] 2. Are there more distinct regional classifications of tropospheric and TTL SHADOZ ozone profiles than the Atlantic-Pacific differentiation identified in *Thompson et al.* [2003a, 2003b]?

[18] In Section 4 comparisons between SHADOZ sondes and OMI-based products are examined. We address the following:

[19] 1. How do total ozone column from the SHADOZ sondes and from OMI compare to one another? How do total ozone from Dobson, Brewer and = System d'Analyse par Observation Zenitale (SAOZ, http://gosic.org/gcos/SAOZ-prog-overview.html) instruments, co-located at six SHADOZ stations, compare to integrated sonde ozone? How do sonde-satellite differences for OMI compare to those for SHADOZ and EP/TOMS [*Thompson et al.*, 2003a, 2007]?

[20] 2. Have station-to-station variations in stratospheric column ozone in 2005–2009 changed since the evaluation of the 1998–2004 SHADOZ record? Do stratospheric ozone profiles during the Aura period indicate instrument bias [*Smit et al.*, 2007; *Deshler et al.*, 2008] as described in T07 for the EP/TOMS period?

[21] 3. A tropospheric ozone residual (column) product, the trajectory-enhanced tropospheric ozone residual (TTOR), based on OMI and MLS, is available on a daily basis through 2011 (*Ziemke et al.* [2006], *Schoeberl et al.* [2007] and updates). How does TTOR compare to sonde integrated ozone at SHADOZ stations?

[22] To answer these questions, ozone profiles from 15 SHADOZ stations that operated in 2005–2009 are analyzed. We summarize operating characteristics of all SHADOZ stations (Section 2). Section 3 starts with an analysis of tropospheric and TTL ozone seasonality over the four newest SHADOZ stations, then presents overall profile ozone, water vapor and temperature climatologies for all 15 SHADOZ stations. Section 4 compares the SHADOZ record with surface-based total ozone at several sites and OMI-based ozone total and TTOR column amounts for 2005–2009. Station biases, identified through total ozone offsets with OMI and stratospheric profile comparisons, are re-assessed and compared to those from EP/TOMS. A summary appears in Section 5.

2. Data and Methods of Analysis

2.1. SHADOZ Methods and Data (2005–2009)

[23] SHADOZ sites are illustrated in Figure 1. Nominally weekly launches, timed for Aura, ERS-2 (European Research Sensing Satellites and ENVISAT overpasses, have produced more than 5000 sets of midday (1000–1400 local time) ozone and PTU profiles since 1998. Table 1 presents station location, operating dates and numbers of soundings from 2005–2009 that are used in our analyses. The Alajuela station has moved several times since late 2005; most data used here are a mixture of profiles from Alajuela and nearby Heredia and are described as Alajuela/Heredia. Data from Hilo, Hawaii, and Hanoi, Vietnam, were added to the SHADOZ archive in 2009 and 2010, respectively.

[24] The ozone measurement is made with electrochemical concentration cell (ECC) ozonesondes [*Johnson et al.*, 2002; *Thompson et al.*, 2000, 2003a]. Temperature, pressure, humidity are recorded by standard radiosondes launched with each ozonesonde. Vaisala RS-80 or RS-92 radiosondes are used at most stations. Exceptions are Réunion and Kuala Lumpur, where a Meteo Modem radiosonde is employed. Ascension and Natal use the Sippican radiosonde, as described at http://croc.gsfc.nasa.gov/shadoz. For comparisons with satellite and ground-based total ozone instruments, data compromised by balloon bursts lower than 20 hPa are not used. Above 10 hPa or burst, extrapolation to total column is made with the new climatology of *McPeters and Labow* [2012]. No normalization to the total ozone of a satellite or ground-based instrument (e.g. Dobson or Brewer) is made. The ozone measuring community continues to evolve standard procedures and to study the sensitivity of the ozone measurement to operating characteristics such as concentration of the sensing solution, background current to which the current that is proportional to the ozone amount is referenced, and to treatment of data in the middle and upper stratosphere [*Smit et al.*, 2011]. Reprocessing of the SHADOZ data is underway and is expected to be complete by 2014. It appears that several stations have modified techniques to be better aligned with the latest WMO recommendations [*Smit et al.*, 2011]. Due to lack of consensus on recommended procedures for higher-than-normal background currents, [*Vömel and Diaz*, 2010; *Stübi and Levrat*, 2010], no adjustments for this parameter have been applied. The more extreme underestimates of TTL and LS ozone attributed to high-background current errors [*Vömel and Diaz*, 2010] affect less than 2% of SHADOZ data and have negligible effect on the statistics presented here.

2.2. Analyses: Tropopause and TTL Definitions and Gravity Wave Index

[25] In the analyses that follow, we refer to the TTL and the tropopause, terms that sometimes vary from one study to another. The TTL is defined as a region in which both tropospheric and stratospheric properties are found in terms of constituent mixing ratios and temperature gradients, wave activity, radiative heating rates and other thermodynamic quantities. A commonly adopted range for the TTL is 14.0 to 18.5 km [*Fueglistaler et al.*, 2009, Figures 1 and 14]; this encompasses the locations of the tropical cold-point tropopause (CPT), the thermal lapse-rate tropopause (LRT) and usually the ozonopause, i.e. a tropopause determined according to an O_3 mixing ratio or gradient.

[26] A detailed discussion of the cold point tropopause (CPT), thermal lapse-rate tropopause (LRT) and ozone-defined tropopause based on SHADOZ data appears in *Sivakumar et al.* [2011] who compute an average of 16.2 ± 0.2 km for the LRT at six southern tropical stations and the same mean (with 0.5 km standard deviation) for a gradient-defined ozonopause (Table 2). For Alajuela/Heredia, the

Table 2. Profile Characteristics of Ozone for Tropical SHADOZ Stations (Within $\pm$ 18 Degrees)

Site	Ozone Minimum Altitude (km)	FT Mean O$_3$ Mixing Ratio (5 km–12 km)	TTL Mean O$_3$ Mixing Ratio (14 km–18.5 km)	Ozonopause (km), LRT (km) (This Study)[a]	Ozonopause (km) [*Sivakumar et al.*, 2011][b]	Mean GWI, Altitude of GW Max.[c]
			Eastern Indian/Western Pacific Oceans			
Kuala Lumpur	13	35.8	120	16.6, 16.9	—	19.4, 17.0
Watukosek	14	30.8	95.6	17.0, 16.9	16.6 $\pm$ 1.3	18.5, 18.1
Fiji	13	40.1	140	16.6, 16.9	16.2 $\pm$ 1.2[d]	12.6, 18.1
Am. Samoa	12	35.7	135	16.5, 17.1	16.4 $\pm$ 0.95	16.1, 18.1
			Equatorial Americas			
San Cristóbal	11	48.1	135	16.5, 16.9	16.6 $\pm$ 1.1	12.6, 18.1
Alajuela/ Heredia	11	48	137	16.3, 17.1	—	—
Paramaribo	11	59	123	15.6, 17.0	—	7.85, 18.1
			Atlantic Ocean and Africa			
Natal	11	58.6	140	16.2, 17.0	15.9 $\pm$ 1.6	10.9, 18.2
Ascension	11	63.9	134	16.2, 17.1	15.5 $\pm$ 1.9	8.35, 18.0
Cotonou	11	72.5	155	15.5, 16.9	—	—
Nairobi	11	55.3	134	16.4, 17.0	16.3 $\pm$ 1.6	16.6, 18.0

[a]Altitude corresponding to 100 ppbv ozonopause as in Figures 6–8; data from 2005–2009.
[b]From ozonopause definition of *Sivakumar et al.* [2011] based on 1998–2008 data. Mean difference between their ozonopause and LRT averages 0.25 km, with five of 7 tropical sites having ozonopause higher than LRT.
[c]GWI = Gravity Wave Index, based on 1998–2007 soundings [*Thompson et al.*, 2011a].
[d]*Sivakumar et al.* [2011] categorizes Fiji as a Sub-tropical site.

analysis by *Selkirk et al.* [2010] of July-August 2005 and 2007 soundings obtained similar tropopauses to those given in *Sivakumar et al.* [2011]. In both cases the tropical CPT is 17.0 ± 0.2 km. The present study uses an ozonopause defined as the altitude at which the mean profile reaches 100 ppbv ozone (Table 2). With few exceptions, the SHADOZ ozone profiles at tropical stations (defined here as within ± 18 degrees latitude) tend to vary monotonically in the TTL, so there is no ambiguity in this definition.

[27] The other parameters used in regional classification of ozone profiles (Section 3.1) are mean ozone mixing ratio in the free troposphere (FT) from 5–12 km (Table 2), mean ozone in the TTL (14.0–18.5 km) and the GWI, that is used as a proxy for the impact of convection on ozone in the FT and TTL. The GWI, based on the formalism of *Teitelbaum et al.* [1994, 1996] with updates by *Pierce and Grant* [1998] and *Thompson et al.* [2010, 2011a], is derived from the frequency of GW occurrence in profiles over the entire dataset at each SHADOZ station [*Thompson et al.*, 2011a]. The GWI was validated during TC4; GW statistics during the July–August 2007 campaign over Alajuela matched climatology.

3. Results: Seasonal and Regional Ozone Profile Climatology

### 3.1. Tropospheric and TTL Ozone Seasonality

[28] Figure 3 displays annual cycles of ozone in the troposphere, TTL and LS for the four newest SHADOZ stations, based on contouring mean monthly-averaged ozone profiles for the years 2005–2009. Because Hanoi and Hilo (Figures 3a and 3b) are the first SHADOZ stations north of 18°N, ozone seasonal cycles for stations south of 18°S, Irene and Réunion (Figures 3c and 3d), are illustrated for comparison.

[29] Sharp ozone gradients in the region encompassing 100 ppbv indicate an LRT and ozonopause (Table 3) over Hanoi above 16 km most of the year (Figure 3a), similar to other Pacific and eastern Indian Ocean SHADOZ sites (Figures 4a–4d). However, Hanoi ozone mixing ratios in the lower troposphere are among the highest of any SHADOZ location due to boundary-layer (BL) pollution in April–May and September–October (60 ppbv or more). In addition, in the springtime (March–April–May, MAM) 80 ppbv ozone in the range from 13 to 16 km is observed, presumably due to stratospheric-to-tropospheric intrusions (S.-Y. Ogino et al., Ozone variations over the northern subtropical region revealed by ozonesonde observations over Hanoi, submitted to *Journal of Geophysical Research*, 2012). Variability in the tropopause region is modulated by large-scale transport associated with the monsoon circulation. Biomass fires may contribute to elevated mid-tropospheric ozone in March–April [*Kondo et al.*, 2004] and during the early monsoon season; note 65–70 ppbv ozone from 8 to 12 km in August (Figure 3a). The pattern of low-moderate ozone air, <40 ppbv, penetrating to 15 km over Hanoi in November–January resembles upper troposphere (UT) and TTL ozone over eastern Indian Ocean and western Pacific SHADOZ sites (Figures 4a and 4b).

[30] The seasonal ozone cross-section over Hilo (Figure 3b) displays similar features to those depicted in *Oltmans et al.* [2004, Figure 2], where more than 400 soundings from 1991–2001 were used for monthly averages. The ozonopause is ∼16 km from August to January; it falls to 13–14 km in MAM as a result of stratospheric influences. In contrast to the March–April UT ozone maxima, distinct ozone minima from 10 to 12 km, ∼35 ppbv, signifying cloud outflow, point to convection in July–October over Hilo as *Oltmans et al.* [2004] noted (Figure 3b [cf. *Oltmans et al.*, 2004, Figure 4]).

[31] Seasonal influences on tropospheric and TTL ozone over Irene and Réunion (Figures 3c and 3d) include a sustained period of biomass burning impacts (August–November) [e.g., *Baldy et al.*, 1996; *Diab et al.*, 1996; *Taupin et al.*, 1999; *Randriambelo et al.*, 2000, 2003; *Thompson et al.*, 2003a, 2003b; *Diab et al.*, 2004; *Clain et al.*, 2009].
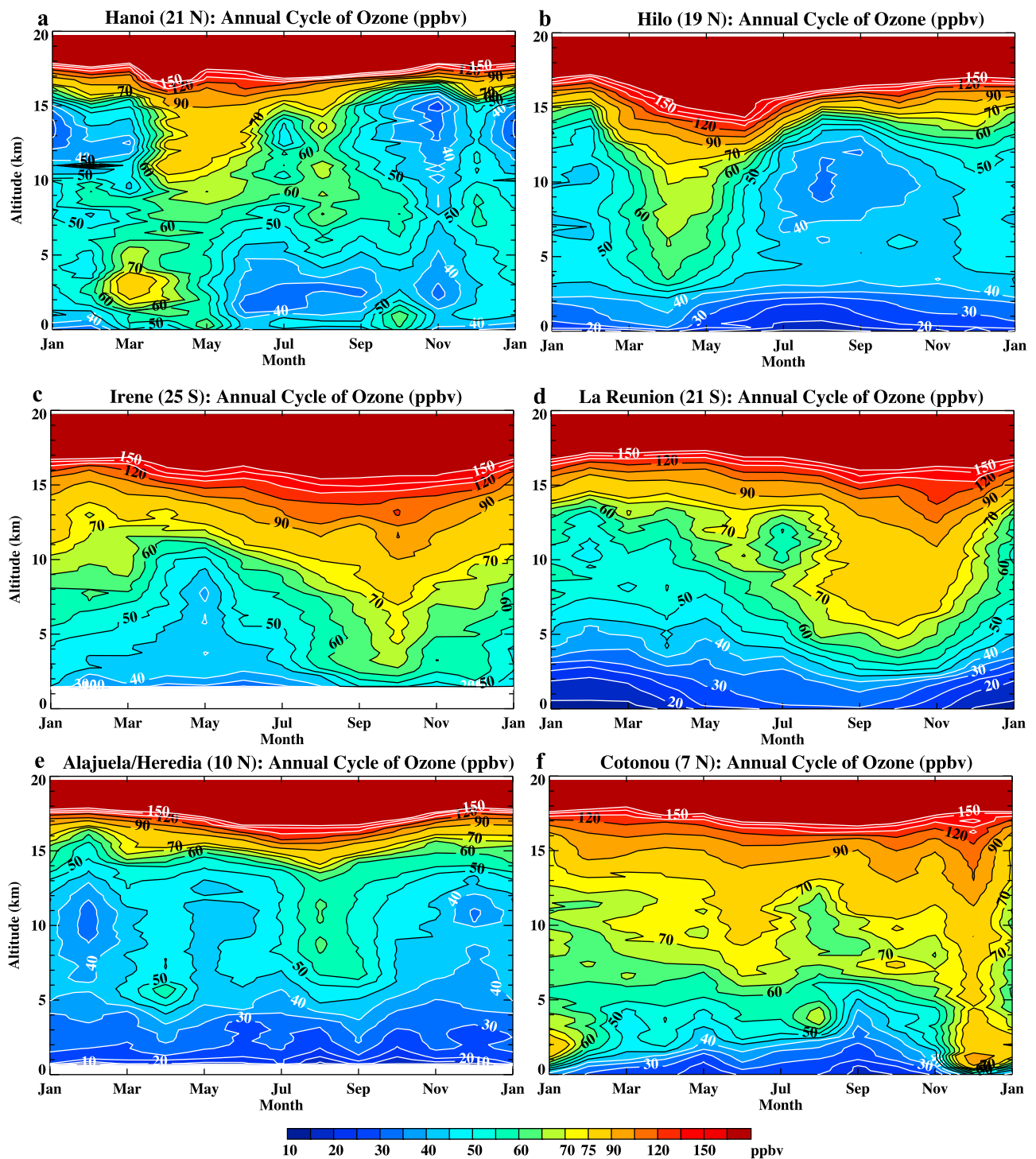
Figure 3. Contours of mean monthly mixing ratio in the troposphere, TTL and LS, 0–20 km, based on monthly averages, 1998–2009: (a) Hanoi (data from 2005–2009), (b) Hilo, (c) Irene, (d) Réunion, (e) Alajuela/Heredia (data from 2006–2009), and (f) Cotonou (data only from 2005–2007). Number of profiles varies, depending on when the station joined (Table 1). Elevated ozone mixing ratios due to pollution, especially from biomass fires, are prominent at all sites except Hilo. Annual cycles of ozone mixing ratios based on 1998–2007 soundings are depicted in *Thompson et al.* [2011a] for Watukosek, Kuala Lumpur, American Samoa, San Cristóbal, and Nairobi and in *Thompson et al.* [2011b] for Ascension Island and Fiji.

Table 3. Characteristics for Sub-tropical SHADOZ Sites

Site	Mean Ozone Mixing Ratio (5–12 km) (ppbv)	Mean Ozonopause (km), LRT (km) (This Study)
Hanoi	53	16.7, 17.4
Hilo, Hawaii	51.2	14.6, 16.9
Irene, South Africa	63	14.1, 17.3
Réunion Island	67.2	14.3, 17.4

Stratosphere-troposphere exchange events over Irene [*Diab et al.*, 1996, 2004] and Réunion [*Baray et al.*, 1998, 1999], the latter frequent occurrences at the edge of the subtropical jet, are well-documented. Tropical cyclones may affect ozone over Réunion [*Leclair de Bellevue et al.*, 2006].

[32] Locally low ozone concentrations, 40–50 ppbv, at 8 km (Irene) and 12 km (Réunion) dominate in May–June (autumn) over Irene (Figure 3c) and December–March (summer) over Réunion (Figure 3d). Ozone pollution from southern African and Madagascar burning affect Irene most heavily from August through November. This is also the time of year with the lowest mean ozonopause and greatest STE (Stratospheric-Tropospheric Exchange) over Irene and Réunion [*Sivakumar et al.*, 2011]. Thus, a single high-ozone feature, 75–105 ppbv, extends from ~4 to 13 km over Irene and from 6 to 13 km over Réunion (Figures 3c and 3d). The Réunion BL is relatively unpolluted, with mixing ratios from 10–30 ppbv (Figure 3d). In September–October–November (SON), BL ozone over Irene averaged 50–60 ppbv, dropping to 40–50 ppbv during December–January–February (DJF). These values were not observed in earlier Irene sondes [*Thompson et al.*, 1996; *Diab et al.*, 2004; *Clain et al.*, 2009]; part of the reason is that Irene launch times in the early 1990s were ~0900 UTC; since 1999 the time has gradually moved to 1500 UTC. An ozone minimum at cloud outflow levels
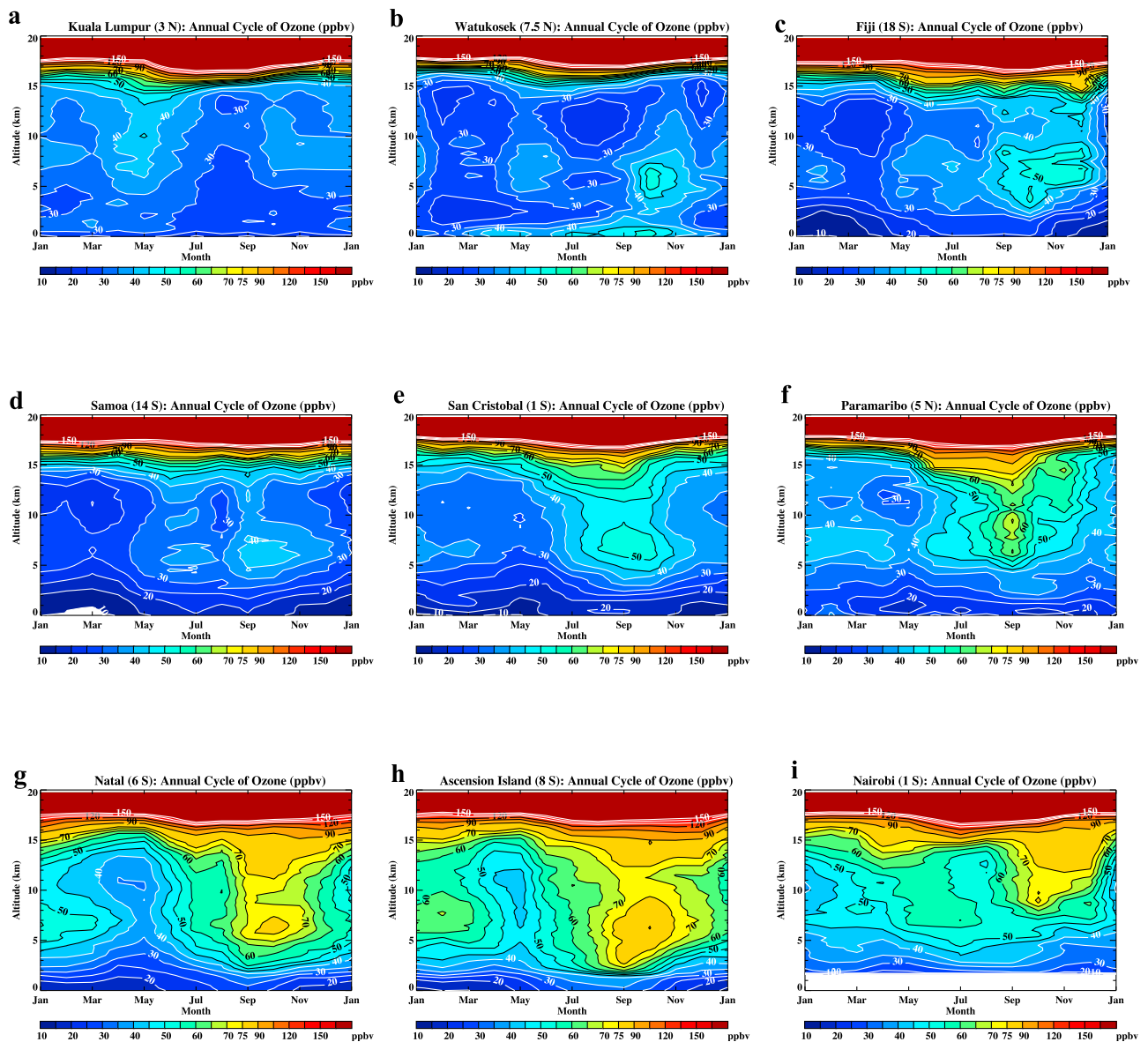
Figure 4. Same as Figure 3 for (a) Kuala Lumpur, (b) Watukosek, (c) Fiji, (d) Samoa, (e) San Cristobal, (f) Paramaribo, (g) Natal, (h) Ascension, and (i) Nairobi.

(10–12 km) is not distinguishable in monthly means (Figure 3c) but low ozone concentrations associated with convection appear in individual Irene profiles (see images at SHADOZ website).

[33] Based on analyses of ozone, water vapor (Cryogenic Frostpoint Hygrometer (CFH) measurements in the TTL and LS) convection and wave activity observed during the NASA TC4 experiment staged from Costa Rica in July and August 2007 [*Selkirk et al.*, 2010], the SHADOZ stations at San Cristóbal, Alajuela/Heredia and Paramaribo are classified as an equatorial Americas region [*Thompson et al.*, 2010], with features distinct from Pacific and Atlantic-African SHADOZ sites. Detailed FT ozone structure visible in the seasonal ozone versus altitude cross-section for Alajuela/Heredia (Figure 3e) is intermediate between San Cristóbal, ~1500 km to the southwest (Figure 4e) and Paramaribo (Figure 4f) [cf. *Peters et al.*, 2004] and Natal to the east (Figure 4g). A mini-dry season occurs over Alajuela/Heredia in April when convection retreats as the ITCZ moves south; the mid-troposphere displays elevated ozone (cf. similar seasonality for Paramaribo in Figure 3f). The ozonopause over Alajuela/Heredia (Figure 3e) is slightly lower (Table 2) than over San Cristóbal (Figure 4e). Near-surface ozone is lower over Paramaribo (10–15 ppbv) than Alajuela/Heredia (20 ppbv, Figure 3e), possibly because the latter is in mountains where a more moderate amount of ozone may result from recirculating pollution. Profiles taken in the Alajuela/Heredia region during the July–August 2007 TC4 campaign by two aircraft fast-response ozone sensors and the sondes showed BL ozone to be <44 ppbv for more than 80% of samples but only about half of the profiles displayed ozone <28 ppbv [*Avery et al.*, 2010].

[34] A shift from mean upward toward downward motion in the Walker circulation leads to a further transition in TTL structure eastward of Paramaribo, as *Peters et al.* [2004] pointed out in comparing Paramaribo, Natal, and Ascension (Figures 4g–4i). Convective signatures over Ascension and Natal are shorter in duration, February–June and MAM, respectively [*Jensen et al.*, 2012], than for equatorial American sites and the Pacific.

[35] The Cotonou soundings in Figure 3f provide the first seasonal picture of the TTL and UT over the east tropical Atlantic; note that the samples cover only 26 months. During most of the year, the ozonopause over Cotonou is between 15 and 16 km (Table 2), about 1 km lower than over Nairobi (Figure 4i). The region encompassed by the 85–100 ppbv ozone gradient over Cotonou extends from 13 to 16 km in every month except January (Figure 3f). This feature is quite different from Ascension and Nairobi (Figures 4h and 4i) and suggests that there is less convective impact over the east tropical Atlantic. The mean ozonopause is 0.5–1.0 km lower at Cotonou than at Ascension and Nairobi (Table 2). The deepest convection and highest ozonopause over Nairobi are at ~17 km in DJF. Although Cotonou ozone concentrations from 6 to 13 km are usually higher than other SHADOZ stations (Table 2), seasonal minima with 60 ppbv ozone in the mid-troposphere occur in January–February and in August (Figure 3f), similar to Nairobi. A thorough discussion of Cotonou ozone seasonality, with context provided by Lagos, Nigeria, MOZAIC (Measurements of Ozone from Airbus In-service Aircraft, http://mozaic.aero.obs-mip.fr/web) landing and takeoff profiles (1998–2004) [*Sauvage*

et al., 2006] and African Monsoon Multidisciplinary Analyses (AMMA) aircraft sampling in July–August 2006, appears in *Thouret et al.* [2009]. Two periods of biomass burning impact are identified, one each in the southern hemisphere (June–July–August (JJA)) and the northern hemisphere (DJF) dry seasons [*Sauvage et al.*, 2007]. The latter, due to fires in the Sahel, influences Cotonou through the Harmattan winds (Figure 3f). Industrial sources may also contribute to Cotonou pollution because Lagos, an urban area with petrochemical emissions, is only 110 km upwind. In JJA, southern hemisphere burning affects the Cotonou soundings, mixing through the ITCZ. The signatures are pronounced between 2 and 5 km [*Thouret et al.*, 2009, Figures 2 and 3]. Pyrogenic origins were confirmed by aircraft sampling from 3–7 degrees N during the AMMA intensive [*Mari et al.*, 2008; *Reeves et al.*, 2010].

[36] The two-season biomass burning effect, with cross-ITCZ transport affecting Cotonou ozone, also influences Ascension. Although there is some convective influence over Ascension in DJF, prior to the main MAM period, the mid-troposphere over Ascension in January and February indicates ozone from fires north of the ITCZ (Figure 4h) (cf. trajectory climatology in *Jensen et al.* [2012]). Pyrogenic effects from northern African burning in ozone soundings made on ship within 350 km of Ascension have also been reported (January–February 1999) [*Thompson et al.*, 2000].

3.2. Ozone Profile Climatologies

[37] Ozone profile climatologies used in BUV satellite algorithms are normally zonally averaged because they were developed when the measurement of stratospheric ozone, approximately 90% of total column ozone, was the principal aim of spaceborne observations. With newer instruments, such as GOME II, SCIAMACHY, and three Aura ozone sensors (MLS, HIRDLS (High Resolution Dynamic Limb Sounder) and OMI on Aura, oriented toward the LS, TTL and UT, better definition of these portions of ozone profiles is required. Early SHADOZ data showed that tropospheric segments of Atlantic and Pacific profiles from typical SHADOZ stations diverge from standard first-guess profiles in the TOMS-OMI algorithm [*Thompson et al.*, 2003b] by 25–50%, depending on season. Recently, Self-Organizing Maps [*Jensen et al.*, 2012] were used to evaluate SHADOZ average profiles as representations for Ascension and Natal (512 Ascension profiles from 1998–2009, 425 for Natal). The MAM and SON means over Ascension and Natal, accounting for 40% of the total profiles, were nearly identical to the minus and plus 1-σ limits of overall mean ozone, respectively. With more extensive subtropical and tropical SHADOZ coverage, we re-examine ozone profiles regionally, beginning with the four subtropical SHADOZ stations.

3.2.1. Subtropical Profiles

[38] Figure 5 summarizes median ozone, temperature and water vapor over the sub-tropical SHADOZ stations, defined as having latitude at 19 degrees or greater: Hanoi, Hilo, Irene, Réunion. The median for ozone is nearly identical to the mean; the maximum and minimum values in Figure 5 correspond, respectively, to the 75th-percentile and 25th-percentile limits for each parameter. The mean ozonopause at Hanoi (Figure 5a) is 16.7 km, 0.7 km lower than the LRT (Table 3); this value for the ozonopause applies throughout the year except for the MAM seasonal drop to ~15 km

Hanoi: 2005-2009

Hilo: 2005-2009

Irene: 2005-2009

La Reunion: 2005-2009
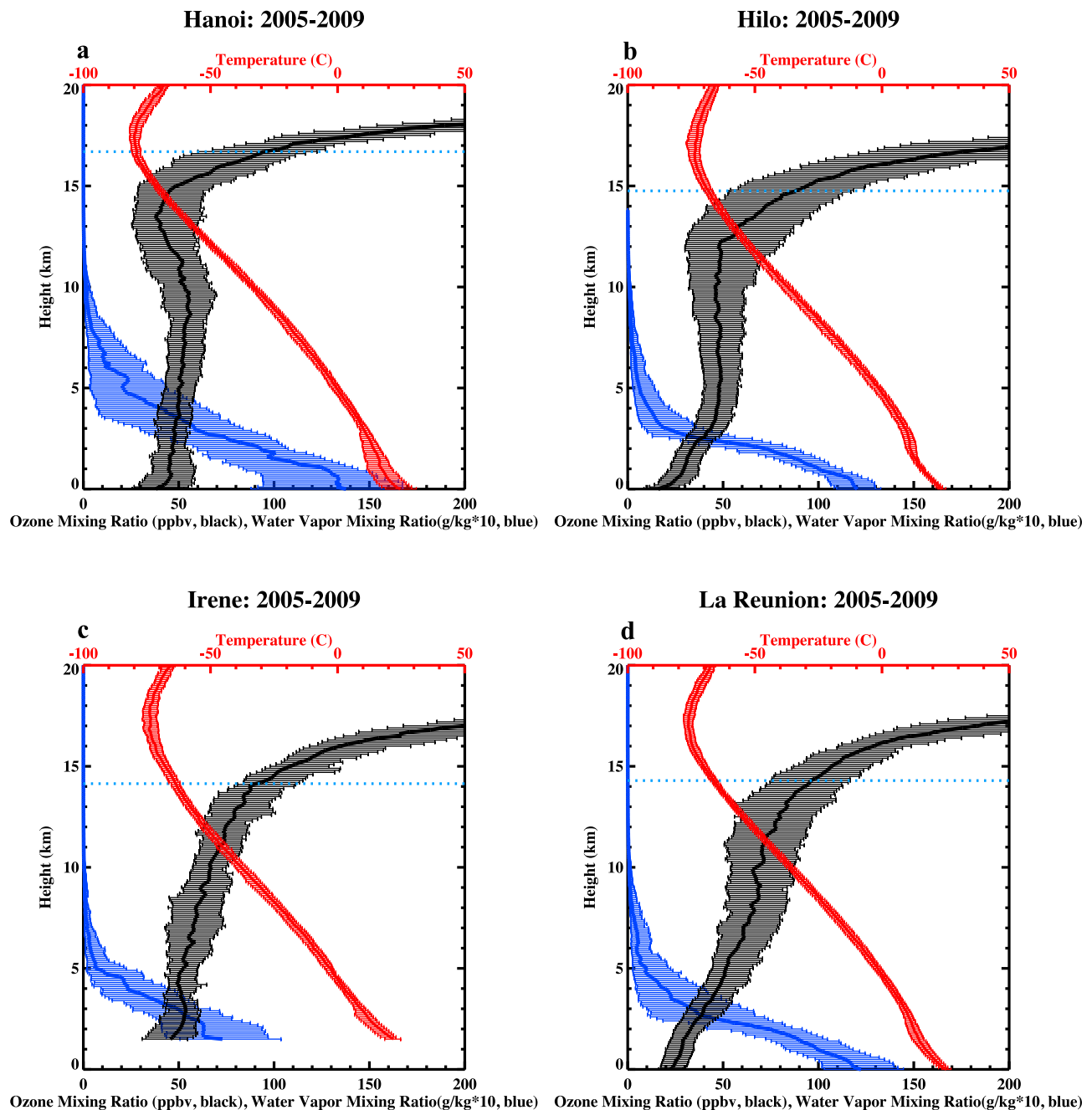
Figure 5. Median ozone, temperature, water vapor profiles, 0–20 km, over SHADOZ subtropical stations, defined as having latitude greater than 18°: (a) Hanoi, Vietnam; (b) Hilo, Hawaii; (c) Irene, South Africa; and (d) La Réunion. The minimum corresponds to the 25th percentile for each parameter; the maximum corresponds to the 75th percentile. Tropopause characteristics, ozonopause and LRT appear in Table 3.

(Figure 3a). The Hanoi mean ozonopause is higher than the other subtropical stations (Table 3) and is similar to the ozonopause for more tropical sites (Table 2; Section 3.2.2 below). Like the eastern Indian Ocean and western Pacific stations, Hanoi displays a relatively low median ozone feature from 13 to 15 km, ~45 ppbv. Over Hilo (Figure 5b), due to a larger impact of MAM STE compared to Hanoi, on average, a distinct local ozone minimum is not observed between 10 km and the TTL. The ozonopause for Irene and

Réunion (Figures 5c and 5d), 14.1 and 14.3 km, respectively, are ~3 km lower than the LRT. This is due to stratospheric influences as discussed above (Figures 3c and 3d). Urban and industrial pollution from the rapidly growing Johannesburg-Pretoria area, interacting with lightning, emissions from biomass fires and highveld coal burning are presumed responsible for the 63 ppbv FT ozone mean over Irene (Table 3 and Figure 5c), along with stratospheric impacts (Figure 3c). Transported pollution from Madagascar
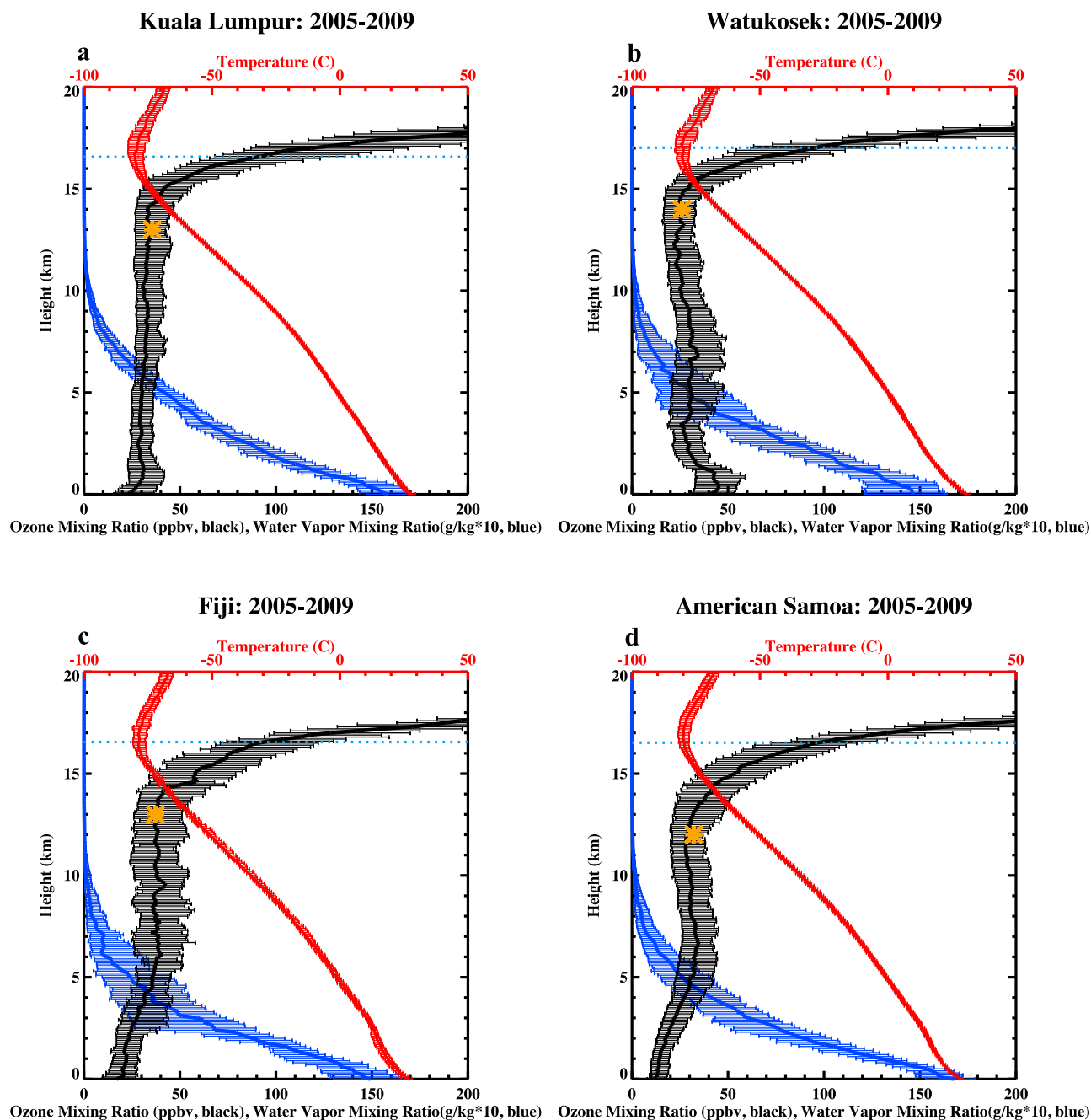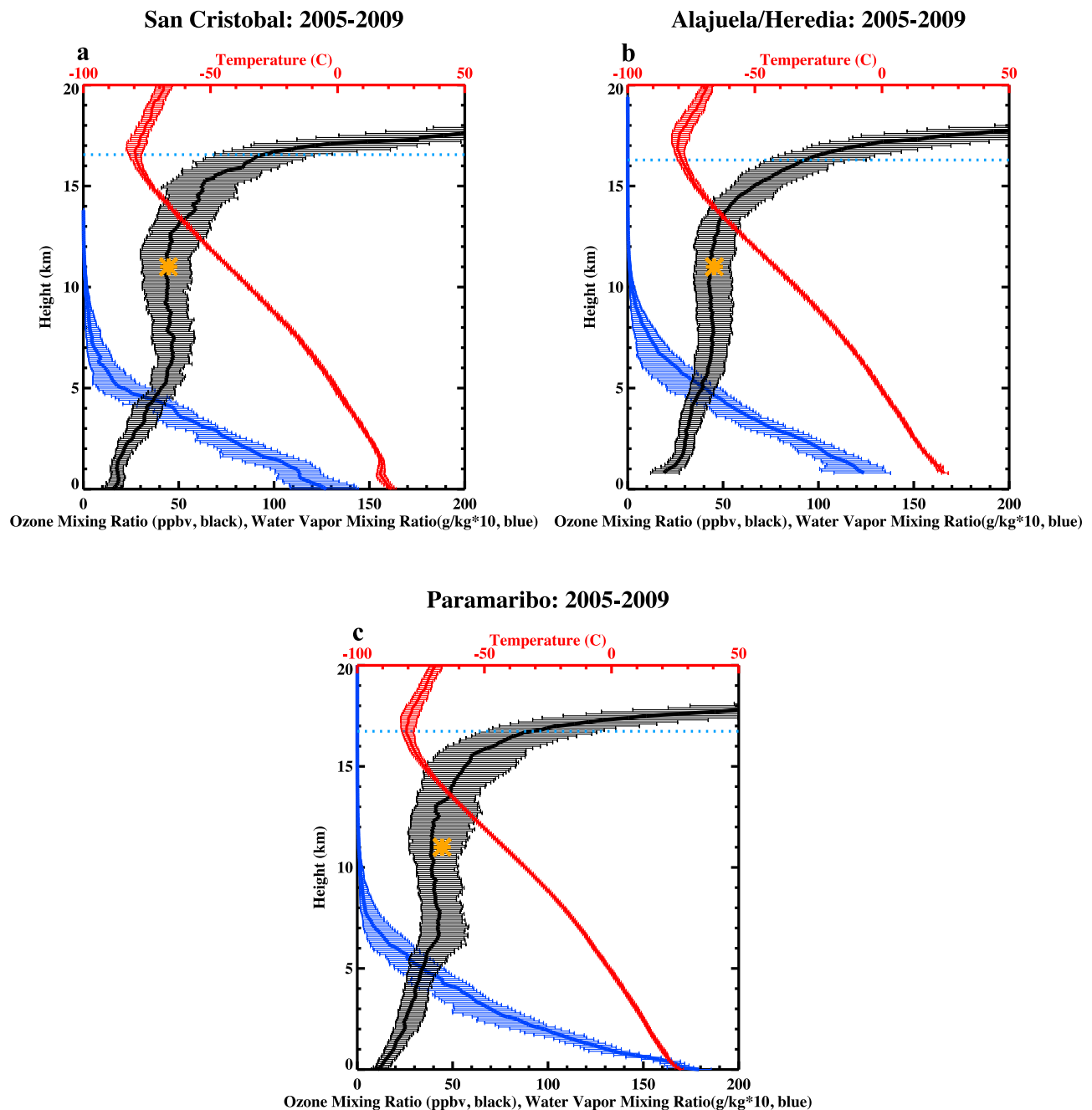
Figure 6. As in Figure 5, the median ozone, temperature, and water vapor profiles over SHADOZ tropical stations within ±18° latitude, in the eastern Indian Ocean, central and western Pacific: (a) Kuala Lumpur, (b) Watukosek, (c) Fiji, and (d) American Samoa. The minimum corresponds to the 25th percentile for each parameter; the maximum corresponds to the 75th percentile. The asterisk locates local minimum O_3 mixing ratio in the UT and TTL, from which location of most prevalent convective outflow inferred. Horizontal dashed line indicates ozonopause (Table 2).

and the mixed southern African influences that affect Irene, signified by a surface mixing ratio of ∼45 ppbv are also associated with high mean ozone over Réunion, 67 ppbv (Table 3 and Figure 5d).

3.2.2. Tropical Ozone Profiles

[39] Figures 6–8 display median ozone, water vapor and temperature profiles for the eleven tropical SHADOZ stations. Table 2 shows a nearly uniform LRT (17.0 ± 0.1 km)

but there is more variation in the ozonopause. The latter parameter, (marked with a dashed horizontal bar, summary in Table 2) falls at 16.2 km, on average, within 0.4 km of the tropopause determined by *Sivakumar et al.* [2011], except at Ascension. In addition to the ozonopause, other parameters used to examine the tropical ozone profiles more closely are summarized in Table 2: the FT mixing ratio; mean TTL ozone mixing ratio (from 14 to 18.5 km); GWI. An

San Cristobal: 2005-2009

Alajuela/Heredia: 2005-2009


Paramaribo: 2005-2009

Figure 7. As in Figures 5 and 6, median ozone, temperature, and water vapor profiles (with limits at 25th and 75th percentile) over SHADOZ stations within the equatorial Americas [*Thompson et al.*, 2010]. (a) For San Cristóbal the degree of convective activity (refer to GWI, Table 2) classifies this more closely to Samoa and Fiji than to Natal and Ascension but FT ozone is distinctly greater over San Cristóbal than the western Pacific. (b) Alajuela/Heredia profile. (c) Likewise, convective activity aligns Paramaribo with Alajuela/Heredia and San Cristóbal but FT ozone is nearly the same as over Ascension and Natal (Figure 8). Asterisks and dashed lines as in Figure 6.

additional parameter is the local minimum ozone mixing ratio in the UT and lower TTL (asterisks in Figures 6–8) that gives rise to an S-shape in the median profile over most stations.

[40] *Eastern Indian Ocean/western Pacific.* In general, Kuala Lumpur, Watukosek, and Fiji, where the deepest tropical convection takes place (Figures 6a–6c) [cf. *Folkins et al.*, 2000, 2002] have one or more local ozone minima from 13 to 15 km; compare the contribution these profiles make to the wave-one ozone feature in zonal cross-section in Figure 15 of *Thompson et al.* [2011b]. The water vapor profiles at all the stations in Figure 6 are fairly similar from the surface to 10 km; in terms of RH, there is a maximum at these sites of 70% at 5 km. The generally high
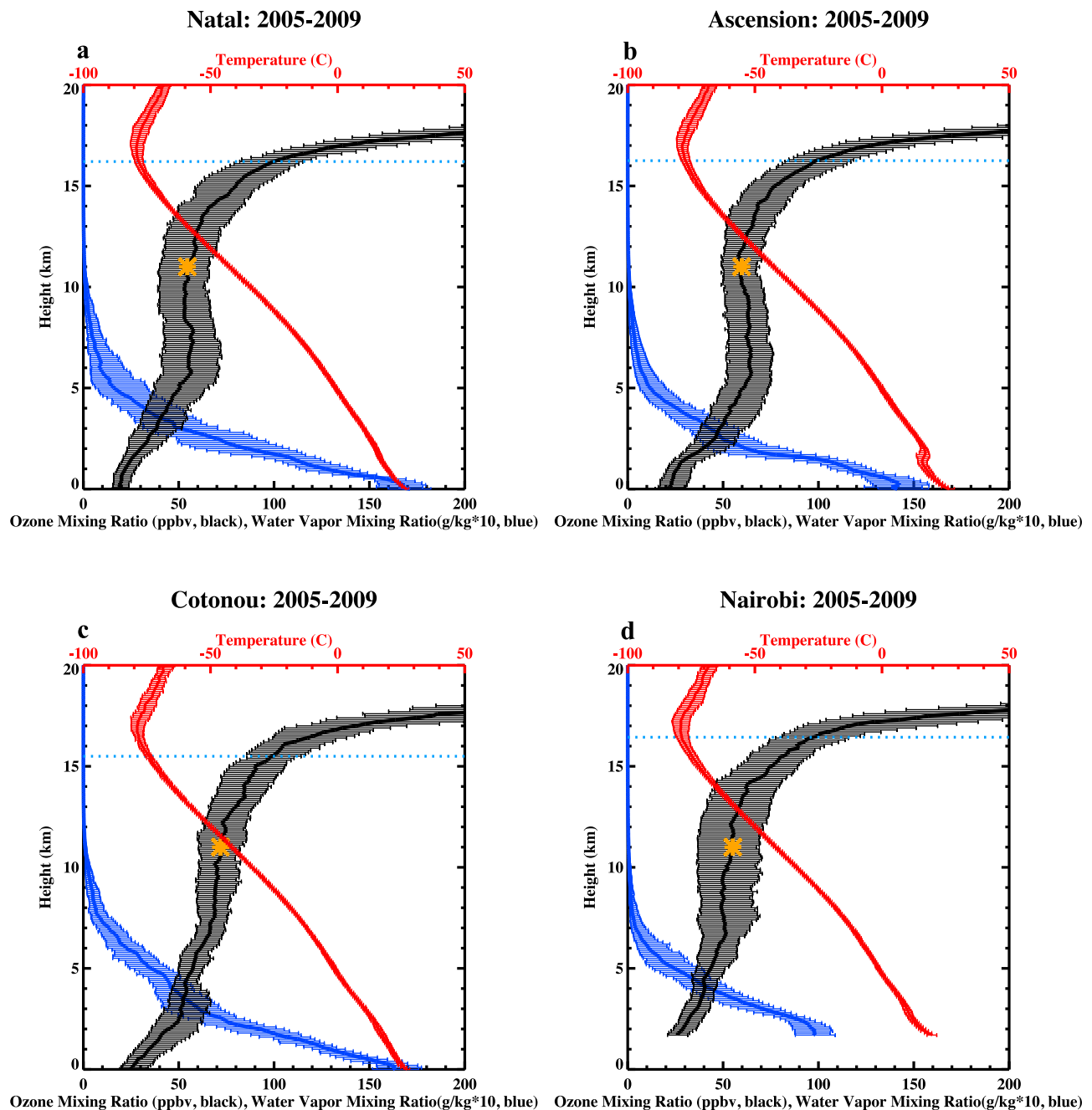
Figure 8. As in Figures 4–6, median ozone, temperature, water vapor profiles over SHADOZ tropical stations in the Atlantic and equatorial Africa: (a) Natal, Brazil; (b) Ascension Island; (c) Cotonou, Benin; and (d) Nairobi. Asterisks and dashed lines as in Figure 6.

levels of convective activity are signified by GWI > 12 (region appears in plain text in Table 2). To the east, at Samoa (Figure 6d), the altitude of minimum ozone drops to 12–13 km.

[41] *Equatorial Americas.* San Cristóbal, Alajuela/Heredia and Paramaribo (Figures 7a–7c) illustrate a transition from the western Pacific to Atlantic [cf. *Peters et al.*, 2004]. The San Cristóbal profile is markedly drier than those over Kuala Lumpur and Watukosek (Figures 6a and 6b), between 5 and 10 km. FT ozone also transitions across the equatorial Americas (Figure 7 and Table 2), with profiles displaying

higher mixing ratios than over the Pacific (Figures 6a–6d), yet lower than over Ascension and Cotonou (Figures 8b and 8c). There appear to be two reasons for this. First, convective influence decreases from western Pacific to Atlantic and Africa (Figure 4) in terms of frequency and duration over the annual cycle. Convective redistribution of ozone appears over Watukosek and Fiji for 7–8 months of the year (Figures 4b and 4c); similar signatures over Natal and Ascension occur only between January or February and May. Thus, the GWI used as an indicator of convective activity (Table 2) is 19 for Kuala Lumpur and Watukosek, 13 for San Cristóbal but only 8–11 at
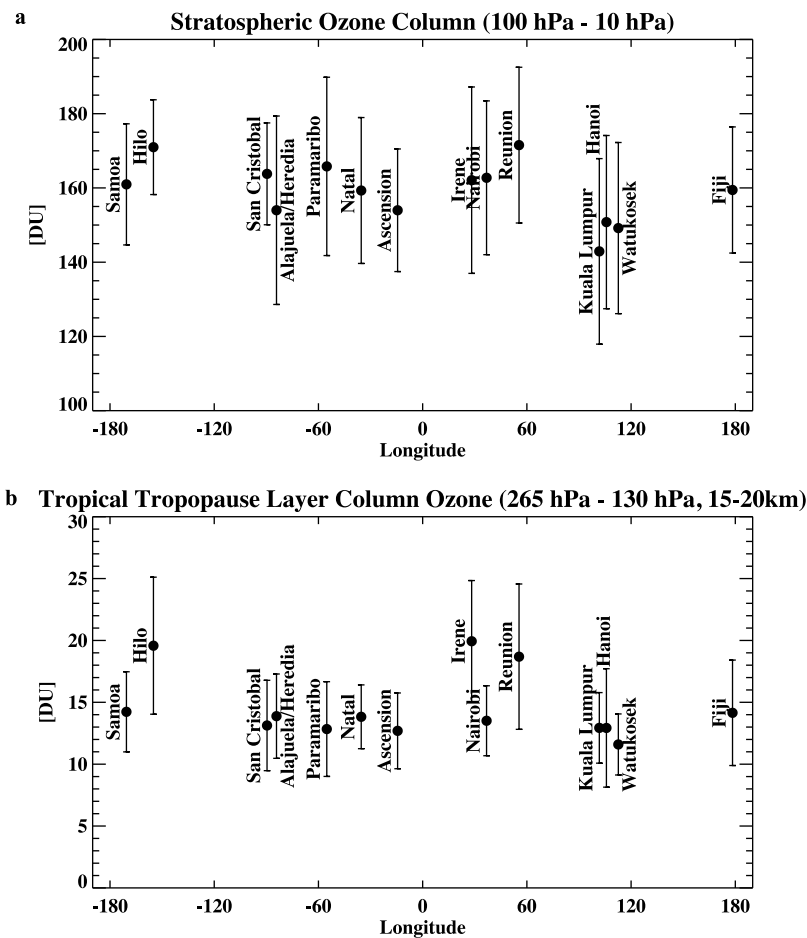
Figure 9. (a) Zonal view of stratospheric column O_3, in Dobson Units (DU, $\pm 1 - \sigma$) determined from integrated stratospheric O_3 of 2005–2009 soundings. (Cotonou not shown due to small number of samples to 10 hPa). Bars indicate $1 - \sigma$ standard deviation. For two subtropical stations, Hilo and Réunion, a column >170 DU may result from intrusion of mid-latitude air parcels. Lack of distinct zonal variation signifies the absence of a wave-one in the stratosphere [cf. *Thompson et al.*, 2007, Figure 6]. (b) Zonal view of integrated column O_3 between 115 and 42 hPa (15–20 km) from same profiles in Figure 9a.

Natal, Paramaribo and Ascension. The ozone minimum, suggesting cloud outflow levels, drops from 13 to 15 km for the western Pacific (asterisks in Figures 6a and 6b) to 11 to 12 km over the equatorial Americas and Atlantic (Figures 7 and 8).

[42] A second factor that reinforces the Pacific toward Africa transition from lower to higher FT ozone is pollution that is more prevalent over the equatorial Americas (Figure 7) than Kuala Lumpur and Watukosek (Figures 6a and 6b). Our studies are not exhaustive [*Oltmans et al.*, 2001], but trajectory climatologies and TC4 case studies [*Avery et al.*, 2010; *Thompson et al.*, 2010] implicate seasonal impacts of biomass burning over the equatorial Americas. In addition, moving from the western Pacific toward a region of subsidence favors persistence of higher ozone in the mid-upper troposphere (cf. the ozone-rich region in Figure 15 of *Thompson et al.* [2011b]), which is evident in Figures 6 and 8. The mean FT ozone mixing ratios measured over San Cristóbal and Alajuela/Heredia are 48 ppbv whereas the eastern Indian Ocean/western Pacific mean ozone falls within 31–40 ppbv.

[43] *Atlantic-Africa.* Parameters for stations in this region appear in Table 2. If decreasing convection and moisture, with intermediate ozone mixing ratios, distinguish the equatorial

Americas from the Pacific, lower pollution and less subsidence differentiate the equatorial Americas (Figure 7) from Natal and Ascension (Figures 8a and 8b). In *Peters et al.* [2004], dominant transport patterns, convection cloud and precipitation distributions were related to tropospheric ozone gradients across San Cristóbal, Paramaribo and Natal. The contribution of biomass fires to a large south Atlantic ozone maximum that affects Natal and Ascension is well-known [*Fishman et al.*, 1991, 1996; *Jacob et al.*, 1996; *Thompson et al.*, 1996]. Lightning over Africa and South America also affects Atlantic ozone [*Thompson et al.*, 2000; *Moxim and Levy*, 2000; *Edwards et al.*, 2003; *Jenkins et al.*, 2003; *Sauvage et al.*, 2006]. Over the continent, biogenic NO [*Jaeglé et al.*, 2004] may add to ozone formation.

[44] Cotonou and Nairobi (Figures 8c and 8d) are both affected by biomass burning from north and south of the ITCZ but Cotonou displays 50% higher ozone from surface to 5 km than Nairobi. Although Cotonou and Nairobi are included in an Atlantic-African category, water vapor profiles diverge for these two sites because Nairobi, 400 km from the Indian Ocean, is semi-arid and Cotonou is coastal. In the FT, Cotonou averages 20 ppbv more ozone than Nairobi (Table 2). The
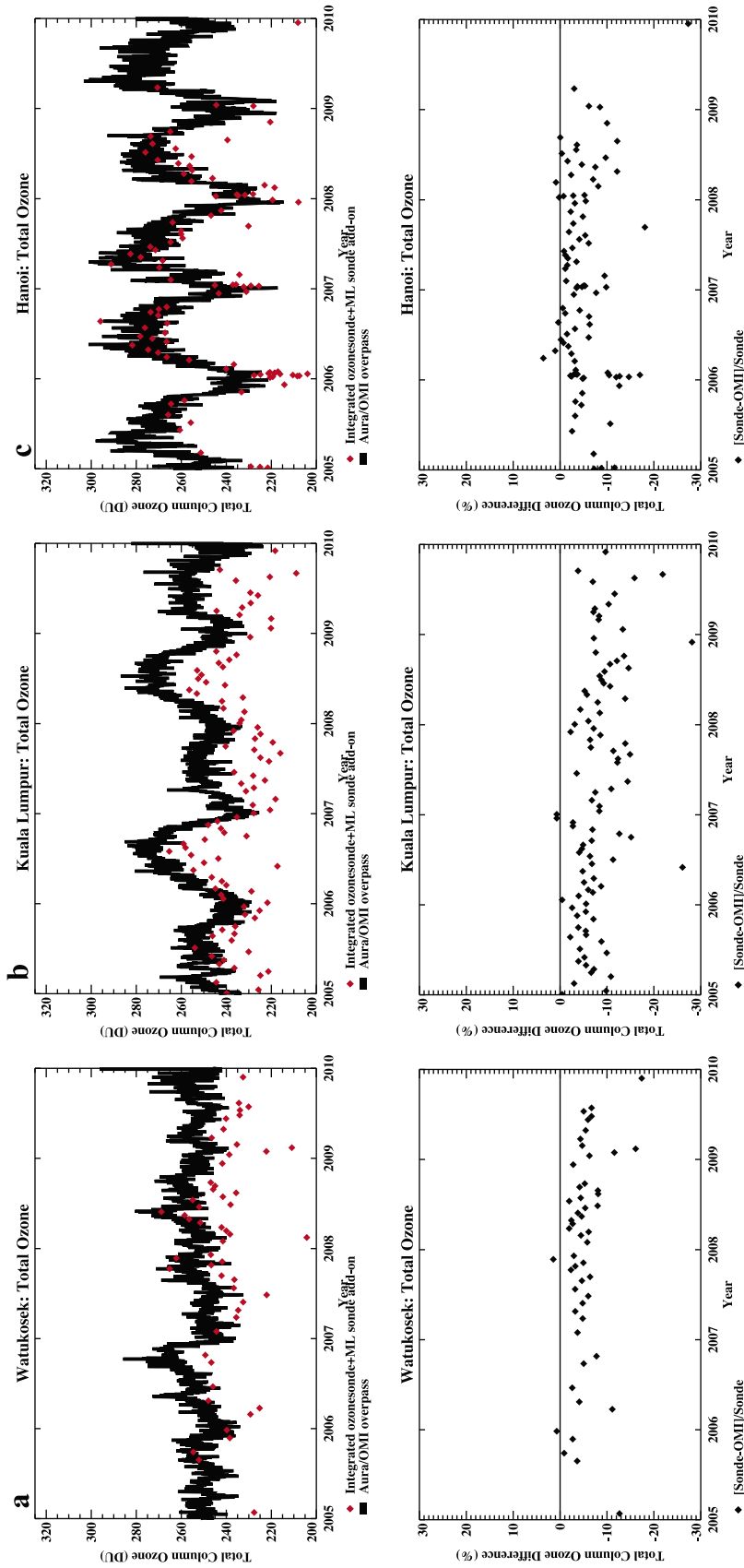
Figure 10. Time-series of OMI overpass total column ozone (solid line) with integrated total column ozone (red) from all soundings in 2005–2009 that reached 20 hPa. Above burst addition to total ozone is from the most recent SBUV/SAGE/MLS climatology [*McPeters and Labow,* 2012]. The latter is similar to *McPeters et al.* [2007] but differs 5–10 DU typically from the SBUV add-on used in earlier EP/TOMS comparisons [*McPeters et al.,* 1997; *Thompson et al.,* 2003a, 2007]. Where available, total O$_3$ from co-located Dobson, Brewer or SAOZ instruments (blue triangle) is given. The lower panel includes sonde-OMI difference and the ground-based-sonde differences. (a) Watukosek; (b) Kuala Lumpur; (c) Hanoi; (d) American Samoa; (e) Hilo, Hawaii; (f) San Cristóbal; (g) Paramaribo; (h) Natal; (i) Ascension; (j) Nairobi; (k) Irene; and (l) Réunion. Due to relatively small sonde datasets, comparisons for Fiji, Alajuela/Heredia and Cotonou are not shown.
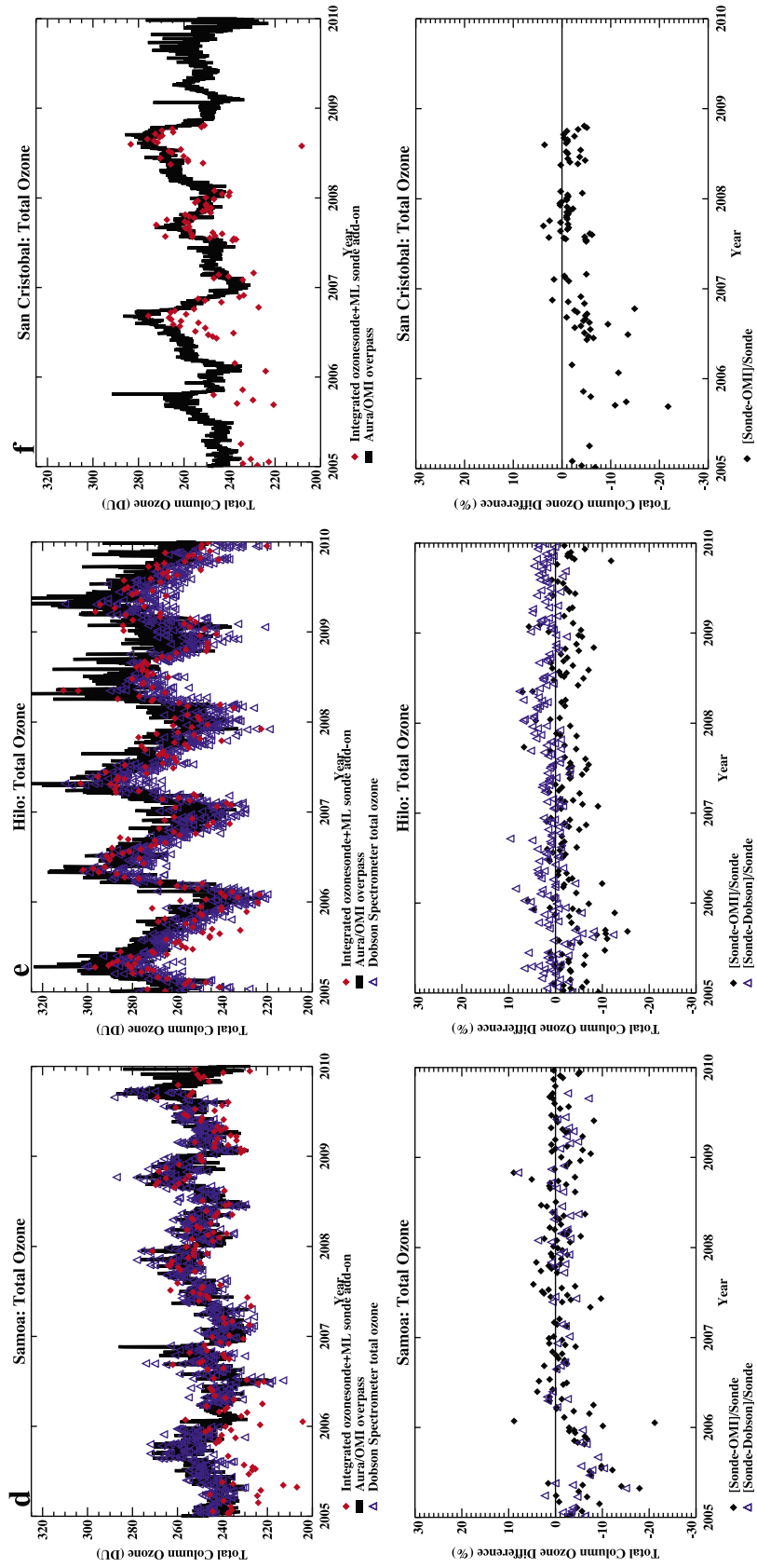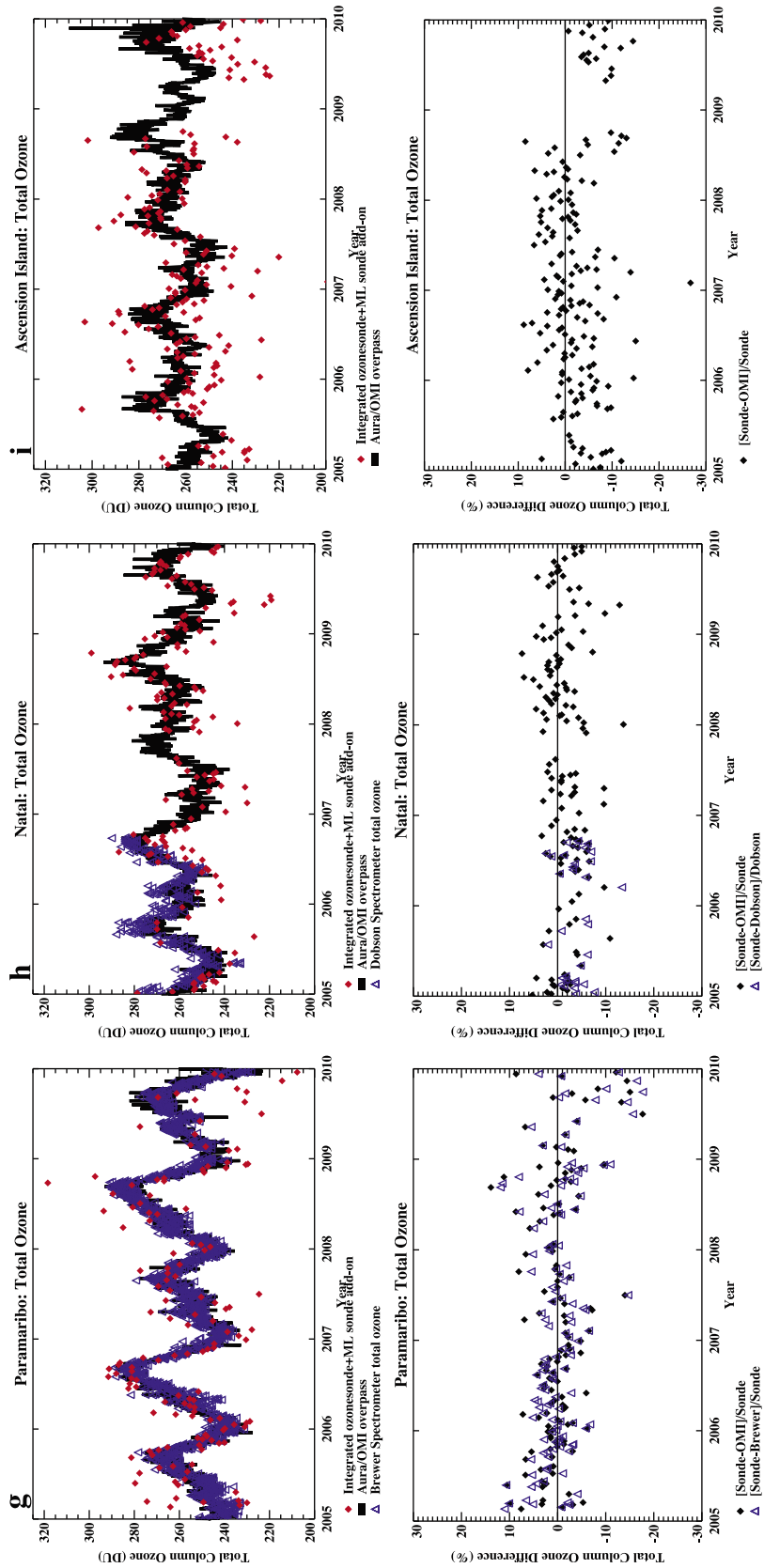
Figure 10. (continued)
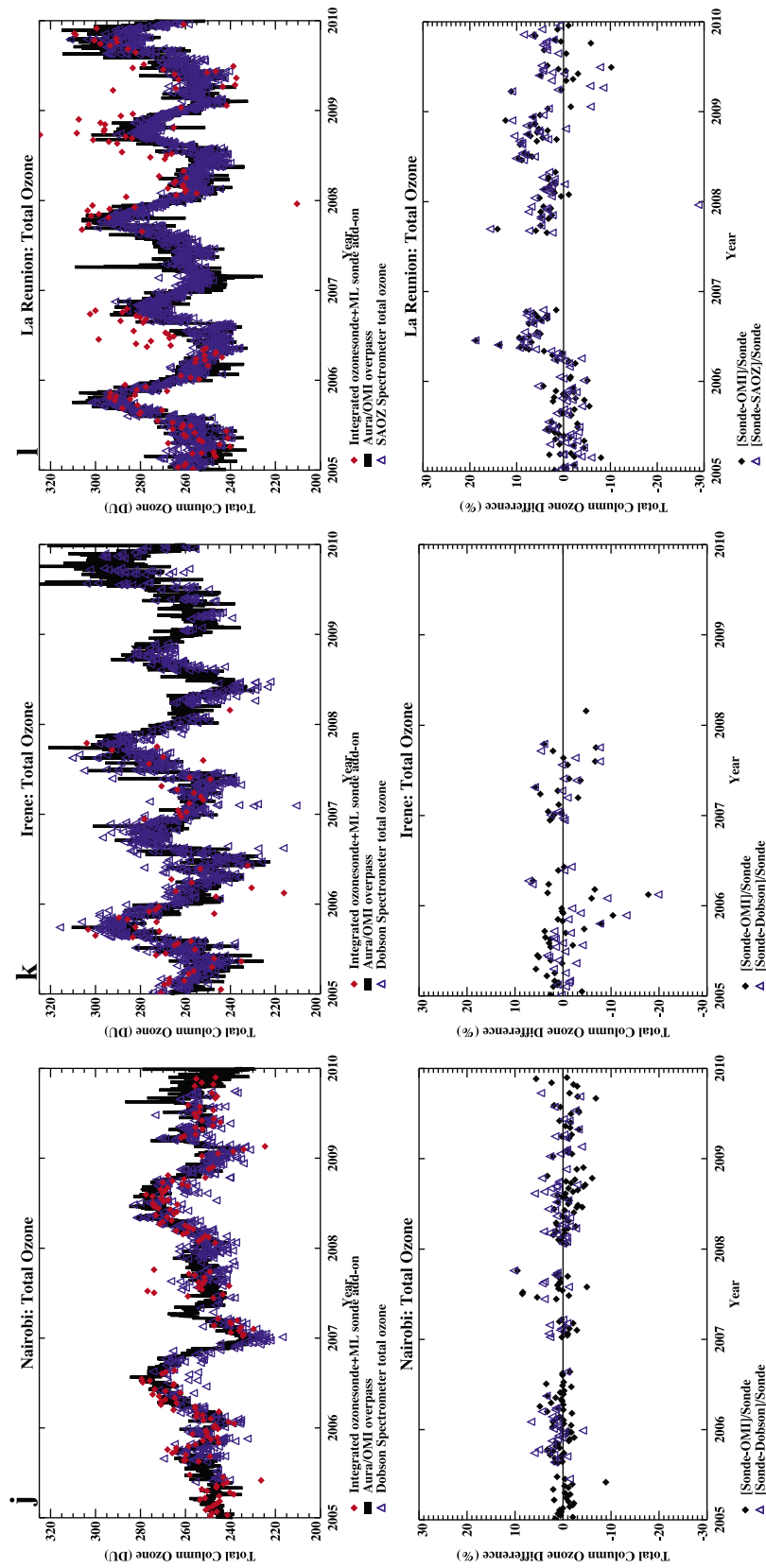
Figure 10. (continued)

Figure 10. (continued)

Longitude Dependence of Difference (sonde-OMI/sonde*100%)
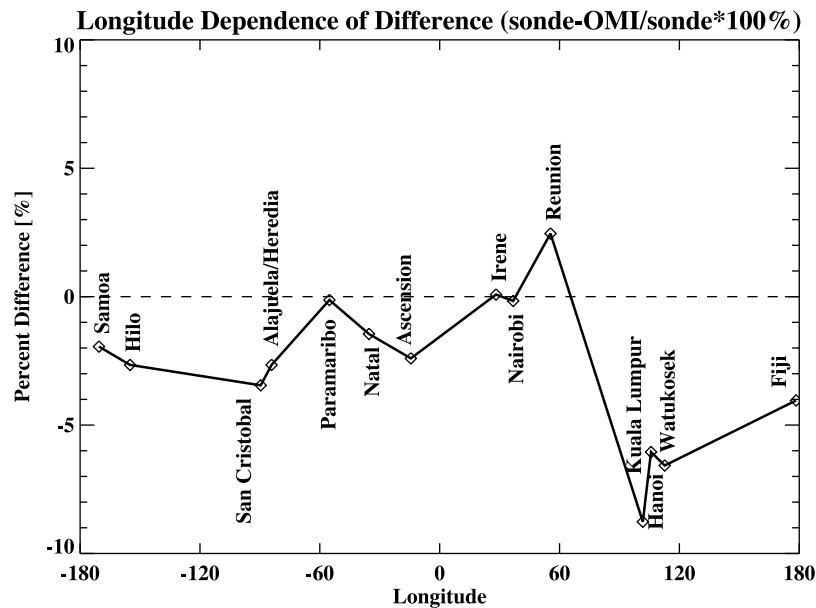

Figure 11. Summary of 2005–2009 sonde total ozone versus OMI overpass column amounts, based on the values illustrated in Figure 10.

reasons for the difference, e.g., larger and more diverse ozone sources over Cotonou or different interactions with convection and regional circulation at each site, have not been explored.

4. Results: Sonde Ozone Columns and Satellite Comparisons and Station Biases

4.1. Stratospheric Comparisons in Column-Integrated Amounts

[45] The "wave-one" pattern in total ozone first described by *Fishman and Larsen* [1987] and *Shiotani* [1992] [cf. *Kim et al.*, 1996, Figure 3] refers to 10–20 Dobson Units (DU) more O_3 column over the Atlantic and eastern Africa compared to the central Pacific where total O_3 is a minimum. The first three years of SHADOZ observations [*Thompson et al.*, 2003a, 2003b] demonstrated that, within the precision of the data, the additional 10–20 DU is tropospheric because there are no statistically significant differences among column-integrated stratospheric ozone over the individual tropical stations. This conclusion holds for the 2005–2009 sondes (Figure 9a) where all stations within ±18° latitude fall within 160 ± 10 DU. That Hilo and Réunion have the two highest stratospheric column ozone amounts reflects their sub-tropical character. Ozone within the TTL over Hilo averages 216 ppbv and the TTL average over Hilo is 194 ppbv. (For the eleven tropical stations TTL ozone averages 131 ±10 ppbv). Individual soundings at Hilo and Réunion as well as at Irene and Hanoi often display an ozonopause below 14 km (Figure 3; cf. the ozonopause and Figure 6 in *Sivakumar et al.* [2011]). Figure 9b, that displays column-integrated TTL and LS ozone (15–20 km), is uniform at the tropical stations, averaging 13–14 DU. Sub-tropical Hilo, Irene, and Réunion average ~20 DU.

4.2. Overpass and Ground-Based Instrument Total Ozone Comparisons

[46] Total ozone comparisons for the 2005–2009 soundings and the coincident OMI overpasses, are shown in Figure 10 for 12 SHADOZ stations, in order from the eastern Indian Ocean eastward through the Americas, Atlantic, Africa and Réunion. All comparisons for which the balloon reached 20 hPa are illustrated. Ozone was integrated from the surface to burst pressure or 10 hPa, whichever is higher, and the most recent MLS-sonde based [*McPeters and Labow*, 2012] climatology added. Note that this extrapolation is nearly identical to *McPeters et al.* [2007]; both those climatologies average ~10 DU higher than the SBUV add-on employed in earlier SHADOZ and TOMS comparisons [*McPeters et al.*, 1997; *Thompson et al.*, 2003a, 2007]. At 7 of the sites shown in Figure 10 independent total ozone measured from the ground is indicated by a Δ symbol. Figure 10 (bottom) displays the difference between total sonde and OMI ozone, referenced to the sonde. As in the 1998–2004 comparisons (T07, Figures 7 and 8), most stations display total ozone from the soundings somewhat lower than OMI. The exception occurs at Réunion after early 2006 (Figure 10l).

[47] The ozone-OMI differences are consistent over time at Hanoi, Hilo, Paramaribo, Natal, Ascension and Irene (Figures 10c and 10f–10l). After 2005 total ozone amounts from three Pacific stations appear to increase slightly, changing offsets at Fiji (not shown due to small sample size), Samoa and San Cristóbal (Figures 10e and 10f), from 5–10% lower than OMI to near agreement. One explanation for this could be a switch in sonde sensing solution type (% KI and buffer amount) at these sites (S. J. Oltmans et al., personal communication, 2010) after evaluation of SHADOZ techniques in the JOSIE-2000 [*Smit et al.*, 2007; *Thompson et al.*, 2007] and BESOS campaigns [*Deshler et al.*, 2008].
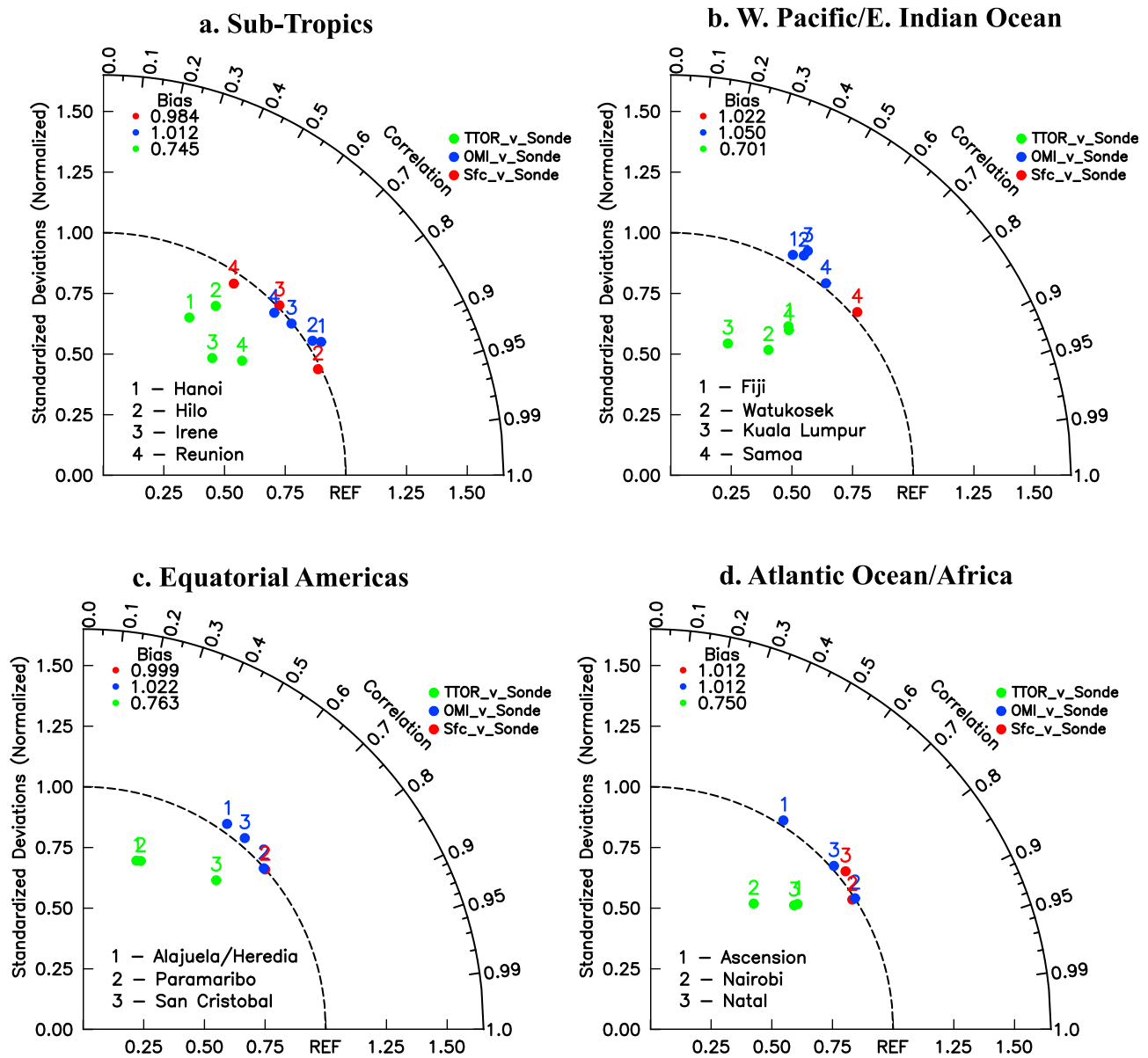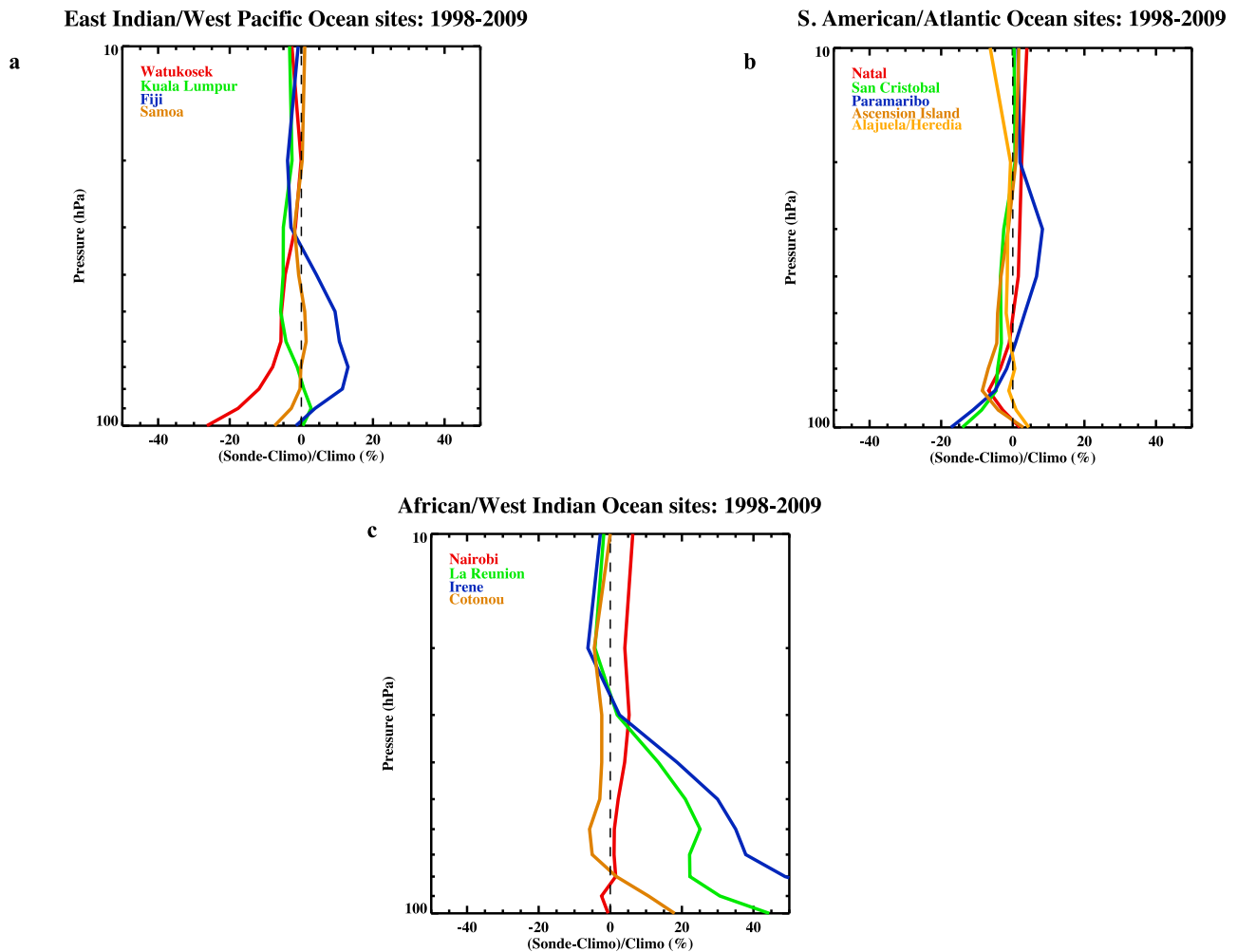
Figure 12. A Taylor diagram, summarizing mean agreement between total ozone from the SHADOZ sondes and OMI total ozone (blue dots) and the sondes and surface total ozone instrument (Dobson, SAOZ or Brewer; red dots); this is based on Figure 10. TTOR-sonde agreement for the ozone column to 200 hPa is given by the green dots (refer to Figure 14). The corresponding radiant amount for each dot is the correlation, representing how well the satellite or ground-based instrument reproduces seasonal and interannual variations in the 2005–2009 time-series. (a) The subtropical SHADOZ stations; the three tropical regions: (b) eastern Indian Ocean/western Pacific, (c) equatorial Americas, and (d) Atlantic-Africa.

4.3. Possible Biases in Total and Stratospheric Ozone

[48] A comparison of mean total ozone column offsets between sondes and overpasses for launch dates during the 2005–2009 OMI period (Figure 11) shows that, on the whole, agreement between the sondes and the satellite is very good, with only 3 stations, Kuala Lumpur, Hanoi and Watukosek, exceeding a 5% absolute difference from the satellite value. This represents a 2–6% improvement over a similar comparison for the SHADOZ sites and overpasses from the 1998–2004 EP/TOMS record (T07, Figure 8) for 5 sites: Fiji, Samoa, San Cristóbal, Natal, Ascension. Why the larger sonde-total ozone discrepancies persist for Kuala Lumpur, Hanoi and Watukosek is not clear. The very low ozone throughout most of the Kuala Lumpur and Watukosek tropospheric profiles (Figures 4a and 4b) corresponds to about 40% of the ozone concentration assumed in the TOMS retrieval algorithm. This disagreement could propagate to a 2–3% overestimate for OMI total ozone. However, that is not the case for Hanoi where much of the mean profile (Figure 3a) resembles the climatology assumed in the retrievals.

East Indian/West Pacific Ocean sites: 1998-2009

S. American/Atlantic Ocean sites: 1998-2009

African/West Indian Ocean sites: 1998-2009

Figure 13. Relative to a mean profile that includes only tropical (within ±18° latitude) SHADOZ profiles from 100–10 hPa, offsets in average profiles from stations in (a) western Pacific and eastern Indian Ocean; (b) equatorial Americas and Atlantic; and (c) Africa and La Réunion. Because data to 10 hPa are sparse for some of the stations illustrated, profiles from 1998–2009 are used.

[49] Figure 12 is a Taylor diagram that depicts total ozone sonde-OMI and sonde-surface total ozone differences in a different manner. For each region (Figures 12a–12d) for which there are sufficient data, the annually averaged offsets of total ozone (OMI in blue, surface instrument in red) are illustrated. The quarter-circle dashed line labeled 1.00 (ordinate) is the Reference (abscissa) that indicates the offsets for OMI total ozone, TTOR or total ozone from the surface instrument relative to the corresponding integrated column from the sonde. From each dot, the corresponding radiant value is a correlation coefficient that incorporates agreement over the time series. Thus, the dots labeled "2" for OMI over Hilo and the nearby Dobson are within 1% of the sonde integrated total ozone with a correlation of 0.84 and 0.88, respectively. For all the stations, annually averaged agreement between OMI and the sondes (and the ground-based instrument and the sondes, where applicable) is excellent, with a mean bias of 1–5% overall (value in upper left of each panel of Figure 12. In general, the OMI discrepancies are greatest for Fiji, Watukosek and Kuala

Lumpur (as in Figure 11) where the correlation (r^2) is only ~0.5. This signifies that seasonality, maximum, and minimum values are less well captured at these stations. Nairobi, Irene and Paramaribo have very good averaged sonde offsets with OMI and Dobson or Brewer, within 0.5%.

[50] In T07 (their Figures 5 and A1) instrument biases determined from the JOSIE-2000 and related campaigns appear to explain some differences among tendencies in stratospheric profiles. To obtain the offsets illustrated in Figure 13, SHADOZ profiles reaching 10 hPa during the 1998–2008 period at the eleven sites in Figures 6–8 were averaged to obtain a mean tropical profile. Means for the individual station profiles were then differenced from this average. Figure 13a shows coherence in the mid-upper stratosphere (above 30 hPa) for all of the eastern Indian Ocean and western Pacific stations, where below 80 hPa differences are assumed to be geophysical. For the eastern Indian ocean-western Pacific sites, offsets are <10% in the 10–30 hPa region; the same holds for the 5 equatorial Americas-Atlantic ozone profiles, except for Paramaribo below 20 hPa (Figure 13b). In Figure 13c the displacement
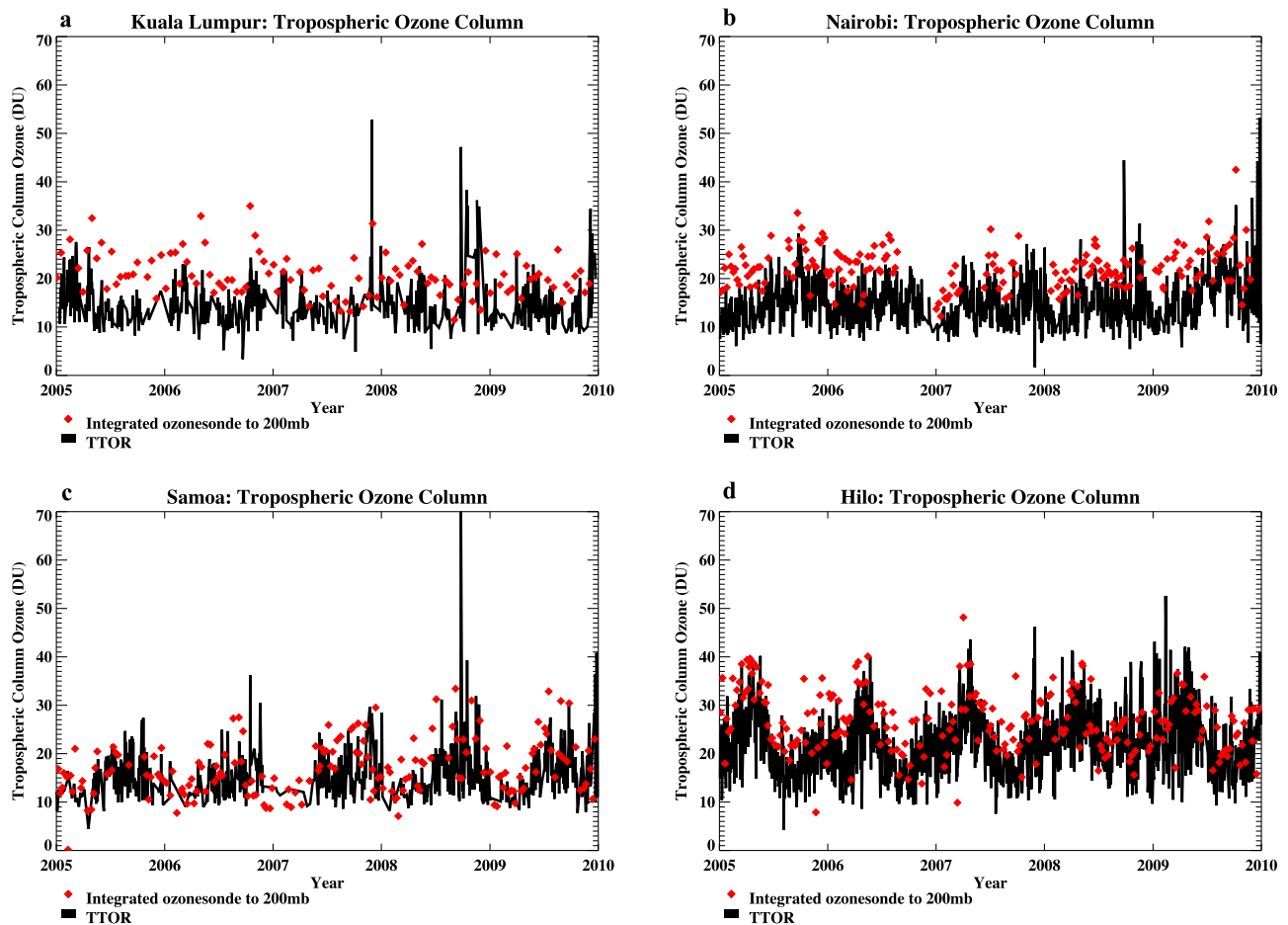
Figure 14. TTOR-sonde offsets for ozone integrated from the surface to 200 hPa: (a) Kuala Lumpur, (b) Nairobi, (c) Samoa, (d) Hilo, (e) Paramaribo, (f) Natal, (g) Ascension, and (h) Reunion.

for sub-tropical Irene and Réunion averages ∼10% in the 10–30 hPa region, but in the LS not surprisingly, Irene and Réunion ozone profiles are much greater than a tropical value. The positive offset from 10–30 hPa over Nairobi (Figure 13c) is similar to the bias noted in T07 that was attributed to the instrument type-sensing solution combination used at that station.

4.4. Comparison of Sondes and TOMS/MLS TTOR Product

[51] Since the launch of Aura, increasing attention has been given to extraction of tropospheric ozone data, mostly through direct observations (Tropospheric Emission Spectrometer (TES, 2004-), MLS [*Jourdain et al.*, 2007; *Logan et al.*, 2008; *Nassar et al.*, 2008; *Osterman et al.*, 2008; *Li et al.*, 2012]), data assimilation with TES, OMI and MLS [*Stajner et al.*, 2008; *Parrington et al.*, 2008, 2009] and variations of residual techniques that are based on subtraction of column amounts. For example, Aura's OMI total ozone and MLS, from which a stratospheric column can be calculated, were used to estimate the tropospheric column [*Ziemke et al.*, 2006, 2011]. A trajectory mapping technique [*Schoeberl et al.*, 2007], that distributes MLS globally and attempts to use a more accurate tropopause, produces a trajectory-enhanced tropospheric ozone residual (TTOR)

product in near-real time. These data are obtained at: <ftp:// hyperion.gsfc.nasa.gov/pub/aura/tropo3>. Because of its OMI heritage and relatively wide usage, the TTOR product is compared to ozone from the 2005–2009 SHADOZ record. We use ozone integrated from the surface to 200 hPa because that is how archived TTOR is reported.

[52] In Figure 14, daily archived TTOR is compared to the sonde column integrated from the surface to 200 hPa at eight SHADOZ stations. The Taylor diagram (Figure 12) is used to illustrate mean agreement and correlations between TTOR and sonde tropospheric ozone (green dots). There is a tendency for the TTOR to be less than the sondes (the mean bias in Figure 12 is ∼25%; the TTOR/sonde-integrated column is ∼0.75, in upper left of each panel). This means that seasonality for some stations is not captured as well as the comparisons with OMI total ozone. The low bias of TTOR was noted by *Schoeberl et al.* [2007] who found that the mean offset for all SHADOZ stations during the initial product evaluation, a 2.5 year period beginning September 2004, was TTOR 2.5 DU less than the corresponding sonde (10–20%). Those values are similar to earlier OMI-MLS products [e.g. *Ziemke et al.*, 2006]. There are several patterns apparent in the comparisons. In Figures 14a and 14b, the TTOR product gives a low column amount, averaging less than 20 DU, with relatively little seasonal or interannual
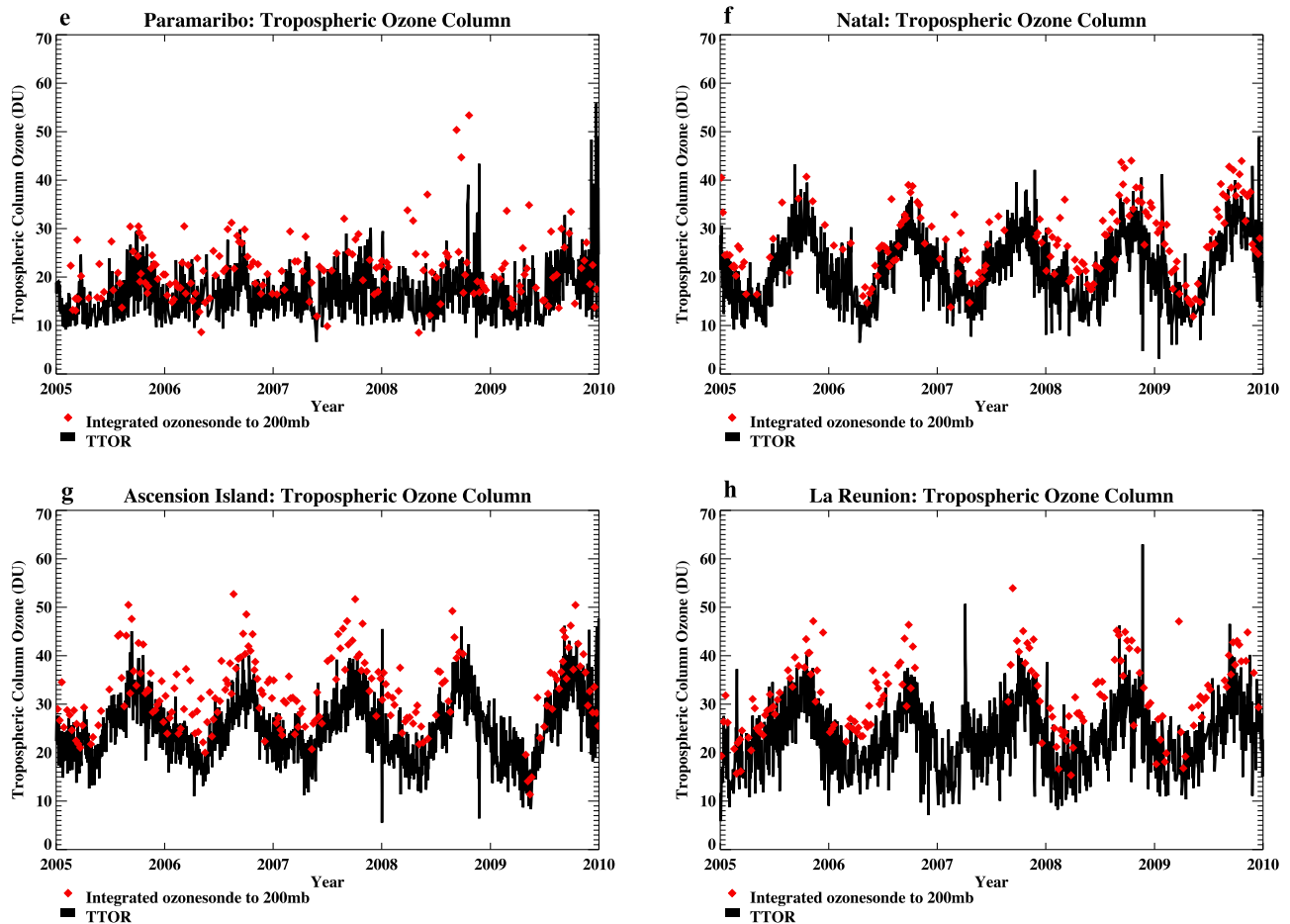
e Paramaribo: Tropospheric Ozone Column

f Natal: Tropospheric Ozone Column

g Ascension Island: Tropospheric Ozone Column

h La Reunion: Tropospheric Ozone Column

Figure 14. (continued)

variation. An exception may have occurred during 2005. Over Kuala Lumpur, both TTOR and sondes (Figure 14a) display higher than average ozone. Likewise, the tropospheric ozone column over Nairobi in both TTOR and sondes was unusually low (Figure 14b). In their respective groupings (Figures 14a and 14b) the Nairobi and Kuala Lumpur discrepancies are relatively high but the correlations, ∼0.6 in both cases, signify reasonably good agreement with the seasonality (Figures 12b and 12d).

[53] The two Pacific stations compared in Figures 14c and 14d, Samoa and Hilo, respectively, appear to display fairly good agreement between TTOR and the sonde tropospheric column. Over Samoa (Figure 14c) there is some missing TTOR data but the annual minimum, February to May, seems to be reproduced in TTOR. The seasonal maximum, when Samoa is affected principally by biomass fires from Africa [*Oltmans et al.*, 2001] and at times from the Indonesian region and Australia, is a strong signal in the June–November period. Thus, over Samoa, TTOR falls ∼25% short of the sonde values. Hilo (Figure 14d) averages 23 DU, which is higher than Samoa; Hilo agreement with TTOR is among the best of the stations.

[54] In the equatorial Americas represented in Figure 14e by Paramaribo, TTOR is ∼0.7 of the sonde value but the correlation (Figure 12c) is <0.3. Paramaribo has relatively small seasonal variations (Section 3.1) that TTOR does not reproduce well. At Natal (Figure 14f) the maximum

tropospheric ozone in August-November averages approximately 3 times the amount of minimum ozone (MAM) when convective impacts are greatest [*Kirchhoff et al.*, 1990; *Jensen et al.*, 2012]. In the second half of the year, ozone is greatly enhanced by transport from African fires [*Logan and Kirchhoff*, 1986], with some contribution from South American burning [*Thompson et al.*, 1996; *Jensen et al.*, 2012]. Overall, TTOR follows the seasonal cycle quite well ($r^2 = 0.77$ in Figure 12d), but it falls short of the sondes throughout the year and has a 25% bias with the sonde-integrated tropospheric ozone. The seasonal cycle of ozone at Ascension (Figure 14g) is not as large as at Natal (factor of 2.5) but the maxima and minima occur at the same time of year [*Olson et al.*, 1996; *Thompson et al.*, 1996; *Jensen et al.*, 2012]. TTOR at Ascension rarely exceeds 40 DU and the mean agreement (Figure 12d) is within ∼30%. The seasonal cycle of tropospheric ozone at Réunion (Figure 14h) resembles that at Ascension and Natal, with transport of pollution from biomass burning a major factor. The variations of the sondes and TTOR at Réunion track one another fairly well (>0.7 correlation in Figure 12a); the agreement with the sondes is similar to that for Ascension and Natal.

[55] A few summary observations emerge from the TTOR-sonde comparisons. First, absolute agreement when the individual profiles are compared is only fair (TTOR ranges from 50–75% of the corresponding sounding). However, correlations at all but 4 SHADOZ stations (Figure 12)

average better than 0.5, which may explain the apparent success of variability studies made with residual-based products (e.g., ENSO or MJO in *Thompson and Hudson* [1999], *Ziemke et al.* [2006, 2010], and *Oman et al.* [2011]). Second, the best seasonal agreement, indicated by the correlation coefficient (Figure 12) is obtained for SHADOZ sites with the highest tropospheric columns and large seasonality (a factor of 2, e.g. Ascension, Natal, Réunion), but also for some of the lowest ozone sites, i.e., Fiji, Samoa. At the same time, these high- and low-ozone stations do not exhibit as good TTOR-sonde agreement overall as Alajuela/Heredia and Paramaribo, two sites with the poorest correlation. One interpretation of these findings: after 20-plus years' experience in creating and analyzing tropospheric ozone residual type products [*Fishman et al.*, 1990], the reasons for more or less accurate column amounts remain poorly understood.

5. Summary

[56] In the first part of this study we presented a regional and seasonal climatology of SHADOZ ozone profiles in the troposphere and TTL based on measurements taken during the early part of the Aura era, 2005–2009. During this period four stations joined SHADOZ for a total of fifteen stations operating from 19°N to 26°S.

[57] For stations operating from 1998 onward, seasonal variations in ozone within the troposphere, TTL and LS are consistent with statistics presented in prior studies with SHADOZ data [*Thompson et al.*, 2003a, 2003b, 2007, 2011a, 2011b]. Here, more detailed comparisons among individual stations are presented in terms of four parameters: ozonopause; FT and TTL mean ozone mixing ratios; Gravity-wave Index as a proxy for convective influence. We find the following.

[58] 1. Two new subtropical stations, Hanoi and Hilo, have stratosphere-troposphere exchange features in common with Réunion and Irene in the southern subtropics. However, Hanoi displays an ozonopause that is ~2 km higher than the other stations and a local ozone minimum just below the TTL that resembles the typical profile of a western Pacific tropical station like Fiji. Hilo displays the least pollution among the subtropical sites. Hanoi and Irene show considerable pollution in the lower troposphere.

[59] 2. Of the eleven tropical stations analyzed, the relatively short-lived Cotonou station (late 2004 to early 2007) showed the greatest tropospheric ozone in the 5–12 km region, 30% more than the other equatorial African site, Nairobi, and more than twice as much as Kuala Lumpur, Watukosek and Samoa. For Cotonou, urban-industrial activities along the Gulf of Guinea may be a nearby ozone source. Northern (DJF) and southern (July–October) biomass fires also contribute to ozone formation over Cotonou, in agreement with regional satellite and profile analyses.

[60] 3. Average features of FT and TTL ozone separate into three tropical zones from west to east: western Pacific and eastern Indian Ocean (Kuala Lumpur, Watukosek, Fiji, Samoa); equatorial Americas (San Cristóbal, Alajuela/Heredia, Paramaribo), the Atlantic and Africa (Natal, Ascension, Cotonou, Nairobi). Within each region, there is a general coherence in ozonopause height, degree of convection inferred from wave activity, and tropospheric pollution.

[61] In the second part of the study, column ozone comparisons are made among SHADOZ stations and total column amounts are compared to OMI (TOMS v8 processed) overpass data, 2005–2009 and to the corresponding TTOR (OMI-MLS residual). Possible biases in stratospheric profiles, based on laboratory studies [*Thompson et al.*, 2007; *Smit et al.*, 2007] and in field tests [*Deshler et al.*, 2008] are re-evaluated.

[62] 4. Stratospheric column amounts, to 10 hPa, and the TTL-LS segment from 265 to 130 hPa (15–20 km), are similar to the earlier SHADOZ record [*Thompson et al.*, 2003a, 2007]. There are no statistically significant differences in the 100–10 hPa-column among the stations within ±18° latitude. Thus, the inference that the zonal wave-one pattern in total ozone [*Fishman and Larsen*, 1987; *Shiotani*, 1992; *Thompson et al.*, 2003a, 2003b] is due not to stratospheric differences but to tropospheric variability in maximum (eastern South America-Atlantic-Africa) and minimum (western Pacific and eastern Indian Ocean) total ozone remains valid.

[63] 5. There is also no variation in the TTL-LS column among the tropical or subtropical stations in the 2005–2009 record. The latter represents an improvement over T07, presumably due to a reprocessing on the Paramaribo data (A. Piters, personal communication, 2011). However, there is a distinct contrast between TTL-LS ozone column amounts (14 DU ± 2 DU) for the 11 tropical stations, and the subtropical sites with 20 ± 2DU.

[64] 6. Total ozone agreement (absolute) between 2005–2009 SHADOZ data and the corresponding OMI columns is better than for the corresponding 1998–2004 total ozone comparisons using EP/TOMS measurements. An updated sonde above-burst extrapolation [*McPeters et al.*, 2007; *McPeters and Labow*, 2012] relative to the EP/TOMS record that adds ~10 DU (3–4% of total column) to the totals may be one reason for the improvement. In three Pacific cases, Samoa, Fiji and San Cristóbal, changes in sonde instrument or sensing solution may also contribute to better agreement.

[65] 7. For the tropical sites, when biases in the individual station profiles from 100 to 10 hPa are examined relative to an all-station ozone mixing ratio, Nairobi appears biased 5% high throughout. This result is unchanged from conclusions in the *Thompson et al.* [2007] analysis of 1998–2004 SHADOZ data.

[66] 8. The TTOR product that is available for daily comparisons, averages 25–30% lower than the sonde integrated column to 200 hPa. However, a moderately high degree of correlation ($r^2 > 0.6$) for all but 4 SHADOZ stations, suggests that seasonal and interannual variations are captured fairly well.

[67] Satellite-based tropospheric ozone products and models suitable for exploring complex variability in the tropics are still in development. We present aspects of the SHADOZ climatology, e.g., seasonal and longitudinal variations in TTL ozone structure, FT layers indicative of pollution and convection, that may highlight factors affecting agreement between the satellite retrieval and coincident ozone profile. Analyses of SHADOZ and TTOR column amounts suggest that we still don't fully understand the reasons for good or bad agreement with the sondes. There remains considerable room for improvement in tropospheric ozone retrievals from satellite. As innovative approaches

evolve with operational sensors and a new generation of ozone satellite instruments is anticipated, tropical ozone soundings will remain essential for algorithm development and evaluation.

References

Avery, M. A., et al. (2010), Convective distribution of tropospheric ozone and tracers in the Central American ITCZ Region: Evidence from observations during TC4, *J. Geophys. Res.*, *115*, D00J21, doi:10.1029/2009JD013450.

Baldy, S., G. Ancellet, M. Bessafi, A. Badr, and D. Lan Sun Luk (1996), Field observation of the vertical distribution of tropospheric ozone at the island of Reunion (Southern Tropics), *J. Geophys. Res.*, *101*, 23,835–23,849, doi:10.1029/95JD02929.

Baray, J. L., G. Ancellet, F. G. Taupin, M. Bessafi, S. Baldy, and P. Keckhut (1998), Subtropical tropopause break as a possible stratospheric source of ozone in the tropical troposphere, *J. Atmos. Sol. Terr. Phys.*, *60*(1), 27–36, doi:10.1016/S1364-6826(97)00116-8.

Baray, J. L., G. Ancellet, T. Randriambelo, and S. Baldy (1999), Tropical cyclone Marlene and stratosphere-troposphere exchange, *J. Geophys. Res.*, *104*(D11), 13,953–13,970, doi:10.1029/1999JD900028.

Bhartia, P. K., R. D. McPeters, L. E. Flynn, S. Taylor, N. A. Kramrova, S. Frith, B. Fisher, and M. DeLand (2012), Solar Backscatter UV (SBUV) total ozone and profile algorithm, *Atmos. Meas. Tech. Discuss.*, *5*, 5913–5951, doi:10.5194/amtd-5-5913-2012.

Burrows, J. P., U. Platt, and P. Borrell (Eds.) (2011), *The Remote Sensing of Tropospheric Composition from Space*, Springer, Heidelberg, Germany, doi:10.1007/978-3-642-14791-3.

Clain, G., J.-L. Baray, R. Delmas, R. Diab, J. Leclair de Bellevue, P. Keckhut, F. Posny, J. M. Metzger, and J. P. Cammas (2009), Tropospheric ozone climatology at two Southern Hemisphere tropical/subtropical sites, (Reunion Island and Irene, South Africa) from ozonesondes, LIDAR, and in situ aircraft measurements, *Atmos. Chem. Phys.*, *9*, 1723–1734, doi:10.5194/acp-9-1723-2009.

Considine, D. B., J. A. Logan, and M. A. Olsen (2008), Evaluation of near-tropopause ozone distributions in the Global Modeling Initiative combined stratosphere/troposphere model with ozonesonde data, *Atmos. Chem. Phys.*, *6*, 1589–1634.

Deshler, T., et al. (2008), Atmospheric comparison of electrochemical cell ozonesondes from different manufacturers, and with different cathode solution strengths: The Balloon Experiment on Standards for Ozonesondes, *J. Geophys. Res.*, *113*, D04307, doi:10.1029/2007JD008975.

Diab, R. D., M. R. Jury, J. Combrink, and F. Sokolic (1996), Vertical ozone distribution over southern Africa and adjacent oceans during SAFARI-92, *J. Geophys. Res.*, *101*, 23,809–23,821, doi:10.1029/95JD01844.

Diab, R. D., A. M. Thompson, K. Mari, L. Ramsay, and G. J. R. Coetzee (2004), Tropospheric ozone climatology over Irene, South Africa from 1990–1994 and 1998–2002, *J. Geophys. Res.*, *109*, D20301, doi:10.1029/2004JD004793.

Edwards, D., et al. (2003), Tropospheric ozone over the tropical Atlantic: A satellite perspective, *J. Geophys. Res.*, *108*(D8), 4237, doi:10.1029/2002JD002927.

Eyring, V., et al. (2005), A strategy for process-oriented validation of coupled chemistry-climate models, *Bull. Am. Meteorol. Soc.*, *86*, 1117–1133, doi:10.1175/BAMS-86-8-1117.

Fishman, J., and J. C. Larsen (1987), Distribution of total ozone and stratospheric ozone in the tropics: Implications for the distribution of tropospheric ozone, *J. Geophys. Res.*, *92*, 6627–6634, doi:10.1029/JD092iD06p06627.

Fishman, J., C. E. Watson, J. C. Larsen, and J. A. Logan (1990), Distribution of tropospheric ozone determined from satellite data, *J. Geophys. Res.*, *95*, 3599–3617, doi:10.1029/JD095iD04p03599.

Fishman, J., K. Fakhruzzaman, B. Cros, and D. Nganga (1991), Identification of widespread pollution in the Southern Hemisphere deduced from satellite analyses, *Science*, *252*, 1693–1696, doi:10.1126/science.252.5013.1693.

Fishman, J., V. G. Brackett, E. V. Browell, and W. B. Grant (1996), Tropospheric ozone derived from TOMS/SBUV measurements during TRACE-A, *J. Geophys. Res.*, *101*, 24,069–24,082, doi:10.1029/95JD03576.

Folkins, I., S. J. Oltmans, and A. M. Thompson (2000), Tropical convective outflow and near-surface equivalent potential temperatures, *Geophys. Res. Lett.*, *27*, 2549–2552, doi:10.1029/2000GL011524.

Folkins, I., C. Braun, A. M. Thompson, and J. C. Witte (2002), Tropical ozone as in indicator of deep convective outflow, *J. Geophys. Res.*, *107*(D13), 4184, doi:10.1029/2001JD001178.

Folkins, I., P. Bernath, C. Boone, K. Walker, A. M. Thompson, and J. C. Witte (2006), The seasonal cycles of O_3, CO and convective outflow at the tropical tropopause, *Geophys. Res. Lett.*, *33*, L16802, doi:10.1029/2006GL026602.

Fu, Q., Y. X. Hu, and Q. Yang (2007), Identifying the top of the tropical tropopause layer from vertical mass flux analysis and CALIPSO lidar cloud observations, *Geophys. Res. Lett.*, *34*, L14813, doi:10.1029/2007GL030099.

Fueglistaler, S., A. E. Dessler, T. Dunkerton, I. Folkins, Q. Fu, and P. W. Mote (2009), The tropical tropopause layer, *Rev. Geophys.*, *47*, RG1004, doi:10.1029/2008RG000267.

Fujiwara, M., K. Kita, and T. Ogawa (1998), Stratosphere-troposphere exchange of ozone associated with the equatorial Kelvin wave as observed with ozonesondes and rawinsondes, *J. Geophys. Res.*, *103*(D15), 19,173–19,182, doi:10.1029/98JD01419.

Fujiwara, M., F. Hasebe, M. Shiotani, N. Nishi, H. Vömel, and S. J. Oltmans (2001), Water vapor control at the tropopause by equatorial Kelvin waves observed over the Galápagos, *Geophys. Res. Lett.*, *28*, 3143–3146.

Gettelman, A., and P. M. D. F. Forster (2002), A climatology of the tropical tropopause layer, *J. Meteorol. Soc. Jpn.*, *80*(4B), 911–924, doi:10.2151/jmsj.80.911.

Intergovernmental Panel on Climate Change (2007), *Climate Change 2007: The Physical Science Basis: Contribution of Working Group I to the Fourth Assessment Report of the Intergovernmental Panel on Climate Change*, edited by S. Solomon et al., Cambridge Univ. Press, Cambridge, U. K.

Jacob, D. J., et al. (1996), Origin of ozone and NO_x in the tropical troposphere: A photochemical analysis of aircraft observations over the South Atlantic basin, *J. Geophys. Res.*, *101*, 24,235–24,250, doi:10.1029/96JD00336.

Jaeglé, L., R. V. Martin, K. Chance, L. Steinberger, T. P. Kurosu, D. J. Jacob, A. I. Modi, V. Yoboué, L. Sigha-Nkamdjou, and C. Galy-Lacaux (2004), Satellite mapping of rain-induced nitric oxide emissions from soils, *J. Geophys. Res.*, *109*, D21310, doi:10.1029/2004JD004787.

Jenkins, G. S., J.-H. Ryu, A. M. Thompson, and J. C. Witte (2003), Linking horizontal and vertical transport of biomass fire emissions to the tropical Atlantic ozone paradox during the Northern Hemisphere winter season: 1999, *J. Geophys. Res.*, *108*(D23), 4745, doi:10.1029/2002JD003297.

Jensen, A. A., A. M. Thompson, and F. J. Schmidlin (2012), Classification of Ascension Island and Natal ozonesondes using self-organizing maps, *J. Geophys. Res.*, *117*, D04302, doi:10.1029/2011JD016573.

Jiang, Y. (2007), Validation of Aura Microwave Limb Sounder ozone by ozonesonde and lidar measurements, *J. Geophys. Res.*, *112*, D24S34, doi:10.1029/2007JD008776.

Johnson, B. J., S. J. Oltmans, H. Voemel, H. G. J. Smit, T. Deshler, and C. Kroeger (2002), Electrochemical concentration cell (ECC) ozonesonde pump efficiency measurements and tests on the sensitivity to ozone of buffered and unbuffered ECC sensor cathode solutions, *J. Geophys. Res.*, *107*(D19), 4393, doi:10.1029/2001JD000557.

Jourdain, L., et al. (2007), Tropospheric vertical distribution of tropical Atlantic ozone observed by TES during the northern African biomass burning season, *Geophys. Res. Lett.*, *34*, L04810, doi:10.1029/2006GL028284.

Kaminski, J., et al. (2008), GEM-AQ, an online global multiscale chemical weather modeling system: model description and evaluation of gas phase chemistry, *Atmos. Chem. Phys.*, *8*, 3255–3281, doi:10.5194/acp-8-3255-2008.

Kim, J.-H., R. D. Hudson, and A. M. Thompson (1996), A new method of deriving time-averaged tropospheric column ozone over the tropics using TOMS radiances: Intercomparison and analysis, *J. Geophys. Res.*, *101*, 24,317–24,330, doi:10.1029/96JD01223.

Kirchhoff, V. W. J. H., I. M. O. da Silva, and E. V. Browell (1990), Ozone measurements in Amazonia: Dry season versus wet season, *J. Geophys. Res.*, *95*(D10), 16,913–16,926, doi:10.1029/JD095iD10p16913.

Kley, D., P. J. Crutzen, H. G. J. Smit, H. Vömel, S. J. Oltmans, H. Grassl, and V. Ramanathan (1996), Observations of near-zero ozone concentrations over the convective Pacific: Effects on air chemistry, *Science*, *274*, 230–233, doi:10.1126/science.274.5285.230.

Komhyr, W. D. (1986), Operations handbook—Ozone measurements to 40 km altitude with model 4A-ECC-ozone sondes, *NOAA Tech. Memo. ERL-ARL-149*, NOAA, Silver Spring, Md.

Komhyr, W. D., R. A. Barnes, G. B. Brothers, J. A. Lathrop, and D. P. Opperman (1995), Electrochemical concentration cell ozonesonde performance evaluation during STOIC 1989, *J. Geophys. Res.*, *100*, 9231–9244, doi:10.1029/94JD02175.

Kondo, Y., et al. (2004), Impacts of biomass burning in Southeast Asia on ozone and reactive nitrogen over the western Pacific in spring, *J. Geophys. Res.*, *109*, D15S12, doi:10.1029/2003JD004203.

Konopka, P., J.-U. Grooß, F. Plöger, and R. Müller (2009), Annual cycle of horizontal in-mixing into the lower tropical stratosphere, *J. Geophys. Res.*, *114*, D19111, doi:10.1029/2009JD011955.

Leclair de Bellevue, J., A. Réchou, J. L. Baray, G. Ancellet, and R. D. Diab (2006), Signatures of stratosphere to troposphere, transport near deep convective events in the southern subtropics, *J. Geophys. Res.*, *111*, D24107, doi:10.1029/2005JD006947.

Lee, S., D. M. Shelow, A. M. Thompson, and S. K. Miller (2010), QBO and ENSO variability in temperature and ozone from SHADOZ (1998–2005), *J. Geophys. Res.*, *115*, D18105, doi:10.1029/2009JD013320.

Li, K.-F., B. Tian, D. E. Waliser, M. J. Schwartz, J. L. Neu, and Y. L. Yung (2012), Vertical structure of MJO-related subtropical ozone variations from MLS, TES, and SHADOZ data, *Atmos. Chem. Phys.*, *12*, 425–436, doi:10.5194/acp-12-425-2012.

Liu, X., P. K. Bhartia, K. Chance, R. J. D. Spurr, and T. P. Kuroso (2010), Ozone profile retrievals from the Ozone Monitoring Instrument, *Atmos. Chem. Phys.*, *10*, 2521–2537, doi:10.5194/acp-10-2521-2010.

Logan, J. A., and V. W. J. H. Kirchhoff (1986), Seasonal variations of tropospheric ozone at Natal, Brazil, *J. Geophys. Res.*, *91*(D7), 7875–7881, doi:10.1029/JD091iD07p07875.

Logan, J. A., D. B. A. Jones, I. A. Megretskaia, S. J. Oltmans, B. J. Johnson, H. Vömel, W. J. Randel, W. Kimani, and F. J. Schmidlin (2003), The quasi-biennial oscillation in equatorial ozone as revealed by ozonesonde and satellite data, *J. Geophys. Res.*, *108*(D8), 4244, doi:10.1029/2002JD002170.

Logan, J. A., I. Megretskaia, R. Nassar, L. T. Murray, L. Zhang, K. W. Bowman, H. M. Worden, and M. Luo (2008), Effects of the 2006 El Niño on tropospheric composition as revealed by data from the Tropospheric Emission Spectrometer (TES), *Geophys. Res. Lett.*, *35*, L03816, doi:10.1029/2007GL031698.

Mari, C. H., G. Cailley, L. Corre, M. Saunois, J. L. Attié, V. Thouret, and A. Stohl (2008), Tracing biomass burning plumes from the Southern Hemisphere during the AMMA 2006 wet season experiment, *Atmos. Chem. Phys.*, *8*, 3951–3961, doi:10.5194/acp-8-3951-2008.

Martin, R. V., et al. (2002), Interpretation of TOMS observations of tropical tropospheric ozone with a global model and in situ observations, *J. Geophys. Res.*, *107*(D18), 4351, doi:10.1029/2001JD001480.

McPeters, R. D., and G. J. Labow (2012), Climatology 2011: An MLS and sonde derived ozone climatology for satellite retrieval algorithms, *J. Geophys. Res.*, *117*, D10303, doi:10.1029/2011JD017006.

McPeters, R. D., G. J. Labow, and B. J. Johnson (1997), A satellite-derived ozone climatology for balloonsonde estimation of total column ozone, *J. Geophys. Res.*, *102*, 8875–8885, doi:10.1029/96JD02977.

McPeters, R. D., G. J. Labow, and J. A. Logan (2007), Ozone climatological profiles for satellite retrieval algorithms, *J. Geophys. Res.*, *112*, D05308, doi:10.1029/2005JD006823.

Mitovski, T., I. Folkins, R. V. Martin, and M. Cooper (2012), Testing convective transport on short time scales: Comparisons with mass divergence and ozone anomaly patterns about high rain events, *J. Geophys. Res.*, *117*, D02109, doi:10.1029/2011JD016321.

Moxim, W. J., and H. Levy II (2000), A model analysis of the tropical South Atlantic Ocean tropospheric ozone maximum: The interaction of transport and chemistry, *J. Geophys. Res.*, *105*(D13), 17,393–17,415, doi:10.1029/2000JD900175.

Nardi, B., et al. (2008), Initial validation of ozone measurements from the High Resolution Dynamic Limb Sounder (HIRDLS), *J. Geophys. Res.*, *113*, D16S36, doi:10.1029/2007JD008837.

Nassar, R., et al. (2008), Validation of Tropospheric Emission Spectrometer (TES) nadir ozone profiles using ozonesonde measurements, *J. Geophys. Res.*, *113*, D15S17, doi:10.1029/2007JD008819.

Olson, J. R., J. Fishman, V. W. J. H. Kirchhoff, D. Nganga, and B. Cros (1996), Analysis of the distribution of ozone over the southern Atlantic region, *J. Geophys. Res.*, *101*(D19), 24,083–24,093, doi:10.1029/95JD03273.

Oltmans, S. J., et al. (2001), Ozone in the Pacific tropical troposphere from ozonesonde observations, *J. Geophys. Res.*, *106*(D23), 32,503–32,525, doi:10.1029/2000JD900834.

Oltmans, S. J., et al. (2004), Tropospheric ozone over the North Pacific from ozonesonde observations, *J. Geophys. Res.*, *109*, D15S01, doi:10.1029/2003JD003466.

Oman, L. D., J. R. Ziemke, A. R. Douglass, D. W. Waugh, C. Lang, J. M. Rodriguez, and J. E. Nielsen (2011), The response of tropical tropospheric ozone to ENSO, *Geophys. Res. Lett.*, *38*, L13706, doi:10.1029/2011GL047865.

Osterman, G. B., et al. (2008), Validation of Tropospheric Emission Spectrometer (TES) measurements of the total, stratospheric and tropospheric column abundance of ozone, *J. Geophys. Res.*, *113*, D15S16, doi:10.1029/2007JD008801.

Parrington, M., D. B. A. Jones, K. W. Bowman, L. W. Horowitz, A. M. Thompson, D. W. Tarasick, and J. C. Witte (2008), Estimating the summertime tropospheric ozone distribution over North America through assimilation of observations from the Tropospheric Emission Spectrometer, *J. Geophys. Res.*, *113*, D18307, doi:10.1029/2007JD009341.

Parrington, M., D. B. A. Jones, K. W. Bowman, A. M. Thompson, D. W. Tarasick, J. Merrill, S. J. Oltmans, T. Leblanc, J. C. Witte, and D. B. Millet (2009), Impact of the assimilation of ozone from the Tropospheric Emission Spectrometer on surface ozone across North America, *Geophys. Res. Lett.*, *36*, L04802, doi:10.1029/2008GL036935.

Peters, W., M. C. Krol, J. P. F. Fortuin, H. M. Kelder, C. R. Becker, A. M. Thompson, J. Lelieveld, and P. J. Crutzen (2004), Tropospheric ozone over a tropical Atlantic station in the Northern Hemisphere: Paramaribo, Surinam (6N, 55W), *Tellus, Ser. B*, *56*, 21–34, doi:10.1111/j.1600-0889.2004.00083.x.

Phahlane, N. A. (2007), Vertical tropospheric ozone structure and associated atmospheric transport over the South African Highveld region, Master's thesis, Univ. of the Witwatersrand, Johannesburg, South Africa

Pierce, R. B., and W. B. Grant (1998), Seasonal evolution of Rossby and gravity wave induced laminae in ozonesonde data obtained from Wallops Island, Virginia, *Geophys. Res. Lett.*, *25*(11), 1859–1862, doi:10.1029/98GL01507.

Randel, W. J., and A. M. Thompson (2011), Interannual variability and trends in tropical ozone derived from SHADOZ ozonesondes and SAGE II satellite data, *J. Geophys. Res.*, *116*, D07303, doi:10.1029/2010JD015195.

Randel, W. J., M. Park, F. Wu, and N. Livesey (2007), A large annual cycle in ozone above the tropical tropopause linked to the Brewer-Dobson circulation, *J. Atmos. Sci.*, *64*, 4479–4488, doi:10.1175/2007JAS2409.1.

Randriambelo, T., J.-L. Baray, and S. Baldy (2000), Effect of biomass burning, convective venting, and transport on tropospheric ozone over the Indian Ocean: Reunion Island field observations, *J. Geophys. Res.*, *105*(D9), 11,813–11,832, doi:10.1029/1999JD901097.

Randriambelo, T., J.-L. Baray, S. Baldy, A. M. Thompson, S. J. Oltmans, and P. Keckhut (2003), Investigation of the short-term variability of tropical tropospheric ozone, *Ann. Geophys.*, *21*, 2095–2106, doi:10.5194/angeo-21-2095-2003.

Reeves, C. E., et al. (2010), Chemical characterisation of the West Africa monsoon during AMMA, *Atmos. Chem. Phys.*, *10*(16), 7575–7601, doi:10.5194/acp-10-7575-2010.

Saiz-Lopez, A., et al. (2011), Climate significance of halogen-driven ozone loss in the tropical marine troposphere, *Atmos. Chem. Phys.*, *11*, 32,003–32,029, doi:10.5194/acpd-11-32003-2011.

Sauvage, B., V. Thouret, A. M. Thompson, J. C. Witte, J.-P. Cammas, P. Nédélec, and G. Athier (2006), Enhanced view of the "tropical Atlantic ozone paradox" and "zonal wave one" from the in situ MOZAIC and SHADOZ data, *J. Geophys. Res.*, *111*, D01301, doi:10.1029/2005JD006241.

Sauvage, B., F. Gheusi, V. Thouret, J.-P. Cammas, J. Duron, J. Escobar, C. Mari, P. Mascart, and V. Pont (2007), Medium-range mid-tropospheric transport of ozone and precursors over Africa: Two numerical case-studies in dry and wet seasons, *Atmos. Chem. Phys.*, *7*, 5357–5370, doi:10.5194/acp-7-5357-2007.

Schoeberl, M. R., et al. (2007), A trajectory based estimate of the tropospheric ozone column using the residual method, *J. Geophys. Res.*, *112*, D24S49, doi:10.1029/2007JD008773.

Selkirk, H. B., H. Vömel, J. M. Valverde Canossa, L. Pfister, J. A. Diaz, W. Fernández, J. Amador, W. Stolz, and G. S. Peng (2010), Detailed structure of the tropical upper troposphere and lower stratosphere as revealed by balloon sonde observations of water vapor, ozone, temperature, and winds during the NASA TCSP and TC4 campaigns, *J. Geophys. Res.*, *115*, D00J19, doi:10.1029/2009JD013209, [printed 116(D10), 2011].

Sherwood, S. C., and A. E. Dessler (2003), Convective mixing near the tropical tropopause: Insights into seasonal variations, *J. Atmos. Sci.*,

60, 2674–2685, doi:10.1175/1520-0469(2003)060<2674:CMNTTT>2.0. CO;2.

Shiotani, M. (1992), Annual, quasi-biennial, and El Niño–Southern Oscillation (ENSO) time-scale variations in equatorial total ozone, *J. Geophys. Res.*, 97(D7), 7625–7633, doi:10.1029/92JD00530.

Sivakumar, V., H. Bencherif, N. Begue, and A. M. Thompson (2011), Tropopause characteristics and variability from 11-year SHADOZ observations in southern tropics and subtropics, *J. Appl. Meteorol. Climatol.*, 50, 1403–1416, doi:10.1175/2011JAMC2453.1.

Smit, H. G. J., and ASOPOS Team (2011), Quality assurance and quality control for ozonesonde measurements in GAW, *WMO/GAW Rep. 201*, World Meteorol. Org., Geneva, Switzerland. [Available at http://www.wmo.int/pages/prog/arep/gaw/documents/GAW_201_30_Sept.pdf.]

Smit, H. G. J., and W. Straeter (2004), JOSIE-1998, Performance of ECC ozone sondes of SPC-6A and ENSCI-Z type, *WMO Global Atmos. Watch Rep. Ser. 157 Tech. Doc. 1218*, World Meteorol. Org., Geneva, Switzerland.

Smit, H. G. J., et al. (2007), Assessment of the performance of ECC-ozonesondes under quasi-flight conditions in the environmental simulation chamber: Insights from the Juelich Ozone Sonde Intercomparison Experiment (JOSIE), *J. Geophys. Res.*, 112, D19306, doi:10.1029/2006JD007308.

Solomon, S., D. W. J. Thompson, R. W. Portmann, S. J. Oltmans, and A. M. Thompson (2005), On the distribution and variability of ozone in the tropical upper troposphere: Implications for tropical deep convection and chemical-dynamical coupling, *Geophys. Res. Lett.*, 32, L23813, doi:10.1029/2005GL024323.

Stajner, I. et al. (2008), Assimilated ozone from EOS-Aura: Evaluation of the tropopause region and tropospheric columns, *J. Geophys. Res.*, 113, D16S32, doi:10.1029/2007JD008863.

Stevenson, D. S., et al. (2006), Multimodel ensemble simulations of present-day and near-future tropospheric ozone, *J. Geophys. Res.*, 111, D08301, doi:10.1029/2005JD006338.

Stübi, R., and G. Levrat (2010), Interactive comment on "Ozone sonde cell current measurements and implications for observations of near-zero ozone concentrations in the tropical upper troposphere," *Atmos. Meas. Tech. Discuss.*, 2, C1252–C1256.

Takashima, H., and M. Shiotani (2007), Ozone variation in the tropical tropopause layer as seen from ozonesonde data, *J. Geophys. Res.*, 112, D11123, doi:10.1029/2006JD008322.

Taupin, F. G., M. Bessafi, S. Baldy, and P. J. Bremaud (1999), Tropospheric ozone above southwestern Indian Ocean is strongly linked to dynamical conditions prevailing in the tropics, *J. Geophys. Res.*, 104(D7), 8057–8066.

Teitelbaum, H., J. Ovarlez, H. Kelder, and F. Lott (1994), Some observations of gravity-wave-induced structure in ozone and water vapour during EASOE, *Geophys. Res. Lett.*, 21(13), 1483–1486, doi:10.1029/93GL02434.

Teitelbaum, H., M. Moustaoui, J. Ovarlez, and H. Kelder (1996), The role of atmospheric waves in the laminated structure of ozone profiles at high latitudes, *Tellus, Ser. A*, 48, 442–455.

Thompson, A. M., and R. D. Hudson (1999), Tropical Tropospheric Ozone (TTO) maps from Nimbus-7 and Earth-Probe TOMS by the modified-residual method: Evaluation with sondes, ENSO signals and trends from Atlantic regional time series, *J. Geophys. Res.*, 104, 26,961–26,975, doi:10.1029/1999JD900470.

Thompson, A. M., K. E. Pickering, D. P. McNamara, M. R. Schoeberl, R. D. Hudson, J. H. Kim, E. V. Browell, V. W. J. H. Kirchhoff, and D. Nganga (1996), Where did tropospheric ozone over southern Africa and the tropical Atlantic come from in October 1992? Insights from TOMS, GTE TRACE A, and SAFARI 1992, *J. Geophys. Res.*, 101(D19), 24,251–24,278, doi:10.1029/96JD01463.

Thompson, A. M., B. G. Doddridge, J. C. Witte, R. D. Hudson, W. T. Luke, J. E. Johnson, B. J. Johnson, S. J. Oltmans, and R. Weller (2000), A tropical Atlantic paradox: Shipboard and satellite views of a tropospheric ozone maximum and wave-one in January–February 1999, *Geophys. Res. Lett.*, 27(20), 3317–3320, doi:10.1029/1999GL011273.

Thompson, A. M., et al. (2003a), Southern Hemisphere Additional Ozonesondes (SHADOZ) 1998–2000 tropical ozone climatology: 1. Comparison with Total Ozone Mapping Spectrometer (TOMS) and ground-based measurements, *J. Geophys. Res.*, 108(D2), 8238, doi:10.1029/2001JD000967.

Thompson, A. M., et al. (2003b), Southern Hemisphere Additional Ozonesondes (SHADOZ) 1998–2000 tropical ozone climatology: 2. Tropospheric variability and the zonal wave-one, *J. Geophys. Res.*, 108(D2), 8241, doi:10.1029/2002JD002241.

Thompson, A. M., J. C. Witte, H. G. J. Smit, S. J. Oltmans, B. J. Johnson, V. W. J. H. Kirchhoff, and F. J. Schmidlin (2007), Southern Hemisphere Additional Ozonesondes (SHADOZ) 1998–2004 tropical ozone climatology: 3. Instrumentation, station-to-station variability, and evaluation with simulated flight profiles, *J. Geophys. Res.*, 112, D03304, doi:10.1029/2005JD007042.

Thompson, A. M., et al. (2010), Convective and wave signatures in ozone profiles over the equatorial Americas: Views from TC4 2007 and SHADOZ, *J. Geophys. Res.*, 115, D00J23, doi:10.1029/2009JD012909, [printed 116(D10), 2011].

Thompson, A. M., A. L. Allen, S. Lee, S. K. Miller, and J. C. Witte (2011a), Gravity and Rossby wave signatures in the tropical troposphere and lower stratosphere based on Southern Hemisphere Additional Ozonesondes (SHADOZ), 1998–2007, *J. Geophys. Res.*, 116, D05302, doi:10.1029/2009JD013429.

Thompson, A. M., et al. (2011b), Strategic ozone sounding networks: Review of design and accomplishments, *Atmos. Environ.*, 45, 2145–2163, doi:10.1016/j.atmosenv.2010.05.002.

Thouret, V., et al. (2009), An overview of two years of ozone soundings over Cotonou as part of AMMA, *Atmos. Chem. Phys.*, 9, 6157–6174, doi:10.5194/acp-9-6157-2009.

Tilmes, S., et al. (2012), Technical Note: Ozonesonde climatology between 1995 and 2011: Description, evaluation and applications, *Atmos. Chem. Phys.*, 12, 7475–7497.

Toon, O. B., et al. (2010), Planning and implementation of the Tropical Composition, Cloud and Climate Coupling Experiment (TC4), *J. Geophys. Res.*, 115, D00J04, doi:10.1029/2009JD013073.

Vömel, H., and K. Diaz (2010), Ozonesonde cell current measurements and implications for observations of near-zero ozone concentrations in the tropical upper troposphere, *Atmos. Meas. Tech.*, 3, 495–505, doi:10.5194/amt-3-495-2010.

Witte, J. C., M. R. Schoeberl, A. R. Douglass, and A. M. Thompson (2008), The Quasi-biennial Oscillation in tropical ozone from SHADOZ and HALOE, *Atmos. Chem. Phys. Discuss.*, 8, 6355–6378, doi:10.5194/acpd-8-6355-2008.

World Meteorological Organization (WMO) (2003), Scientific Assessment of Ozone Depletion: 2002, *Rep. 47*, 498 pp., Global Ozone Res. and Monit. Proj., Geneva, Switzerland.

World Meteorological Organization (WMO) (2007), Scientific Assessment of Ozone Depletion: 2006, *Rep. 50*, 572 pp., Global Ozone Res. and Monit. Proj., Geneva, Switzerland.

World Meteorological Organization (WMO) (2011), Scientific Assessment of Ozone Depletion: 2010, *Rep. 52*, 516 pp., Global Ozone Res. and Monit. Proj., Geneva, Switzerland.

Yonemura, S., H. Tsuruta, S. Kawashima, S. Sudo, L. C. Peng, L. S. Fook, Z. Johar, and M. Hayashi (2002), Tropospheric ozone climatology over Peninsular Malaysia from 1992 to 1999, *J. Geophys. Res.*, 107(D15), 4229, doi:10.1029/2001JD000993.

Zachariasse, M., H. G. J. Smit, P. F. J. van Velthoven, and H. Kelder (2001), Cross-tropopause and interhemispheric transports into the tropical free troposphere over the Indian Ocean, *J. Geophys. Res.*, 106(D22), 28,441–28,452, doi:10.1029/2001JD900061.

Ziemke, J. R., S. Chandra, B. N. Duncan, L. Froidevaux, P. K. Bhartia, P. F. Levelt, and J. W. Waters (2006), Tropospheric ozone determined from aura OMI and MLS: Evaluation of measurements and comparison with the Global Modeling Initiative's Chemical Transport Model, *J. Geophys. Res.*, 111, D19303, doi:10.1029/2006JD007089.

Ziemke, J. R., S. Chandra, L. D. Oman, and P. K. Bhartia (2010), A new ENSO index derived from satellite measurements of column ozone, *Atmos. Chem. Phys.*, 10, 3711–3721, doi:10.5194/acp-10-3711-2010.

Ziemke, J. R., S. Chandra, G. J. Labow, L. Froidevaux, and J. C. Witte (2011), A global climatology of tropospheric and stratospheric ozone derived from Aura OMI and MLS measurements, *Atmos. Chem. Phys.*, 11, 9237–9251, doi:10.5194/acp-11-9237-2011.